CRREL REPORT 95-5

# Initial Analyses of Eagle River Flats Hydrology and Sedimentology, Fort Richardson, Alaska

Daniel E. Lawson, Susan R. Bigl, John H. Bodette and Patricia Weyrick

March 1995

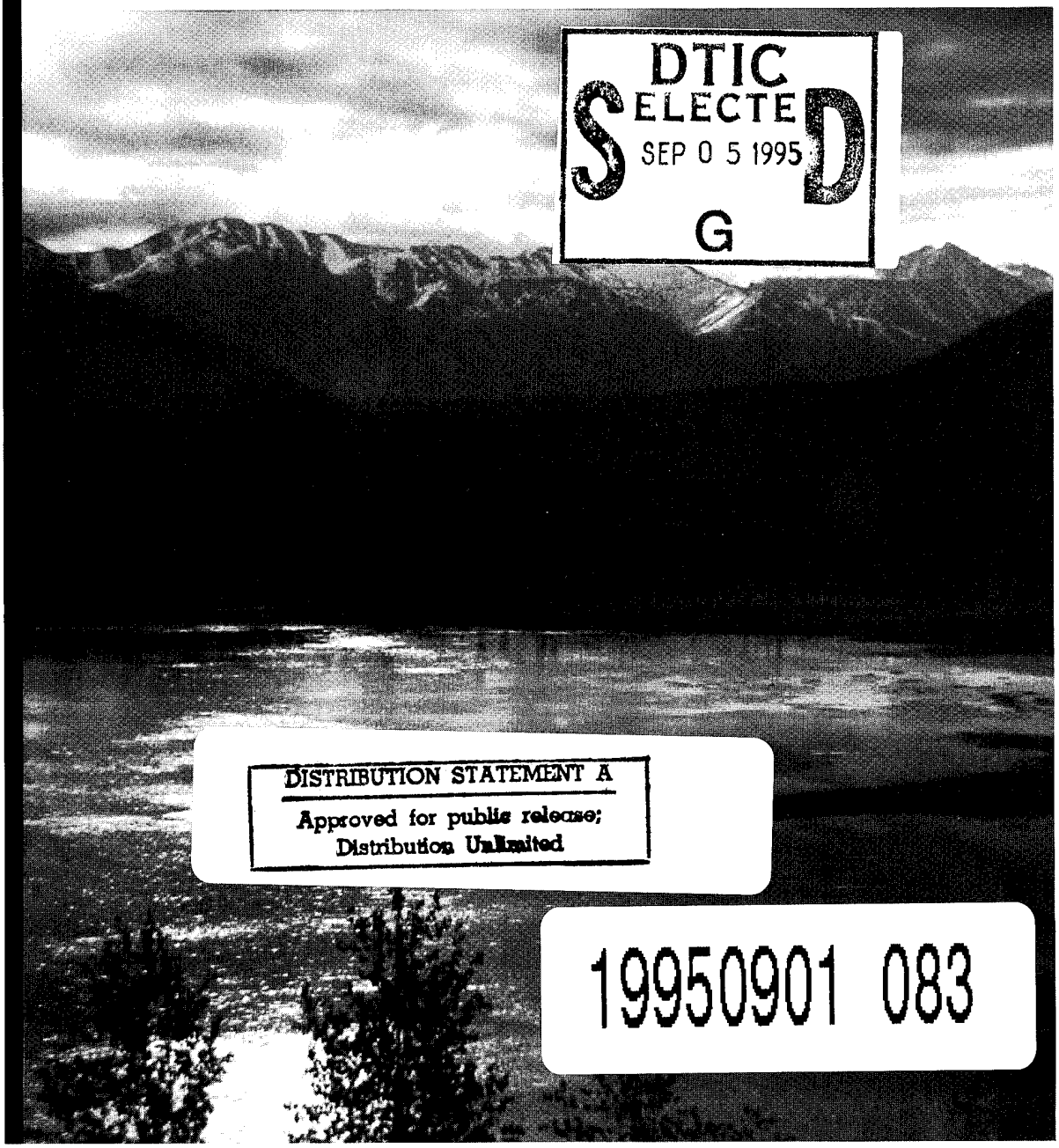

***Abstract***

The physical environment of Eagle River Flats (ERF), a subarctic tidal flat and salt marsh, is progressively changing because of the interactions of multiple physical processes, including a high tidal range, two primary sediment sources, cold climate and location within an active earthquake zone. In addition, ERF has been used by the U.S. Army as an artillery range, where high explosives or smoke-producing shells have been detonated, causing cratering and disrupting drainage. The physical environment of ERF needs to be understood to help remediate a problem of unusually high mortality rates in migrating waterfowl. This high mortality of ducks is attributable to ingestion of elemental white phosphorus (P4) particles (from smoke-producing devices), which are now distributed within near-surface sediments of the ponds and marshes. The complexity of this dynamic environment makes it extremely difficult to predict what physical effects remedial measures for the $P_4$ contamination will have and, conversely, what short- and long-term effects the physical system will have on the effectiveness and success of proposed remedies. Understanding both the system's response and the effects of remedial technologies is critical to deciding what measures are used. This report presents the initial analysis of the physical processes of erosion, sedimentation and sediment transport and the factors controlling their activity within a portion of ERF.

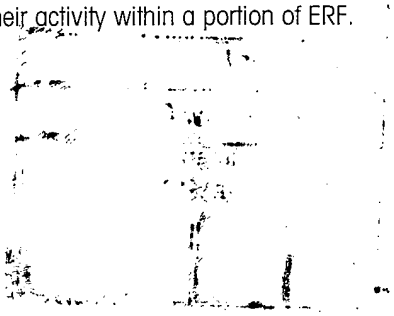

*Cover: Peak tidal flooding inundates innermost pond areas of Eagle River Flats. Area B, located in Figure 2 of text, is shown during peak flooding event during May 1994.*

For conversion of SI metric units to U.S./British customary units of measurement consult *Standard Practice for Use of the International System of Units (SI)*, ASTM Standard E380-89a, published by the American Society for Testing and Materials, 1916 Race St., Philadelphia, Pa. 19103.

CRREL Report 95-5

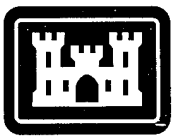

**US Army Corps of Engineers**
Cold Regions Research & Engineering Laboratory

# Initial Analyses of Eagle River Flats Hydrology and Sedimentology, Fort Richardson, Alaska

Daniel E. Lawson, Susan R. Bigl, John H. Bodette and Patricia Weyrick

March 1995

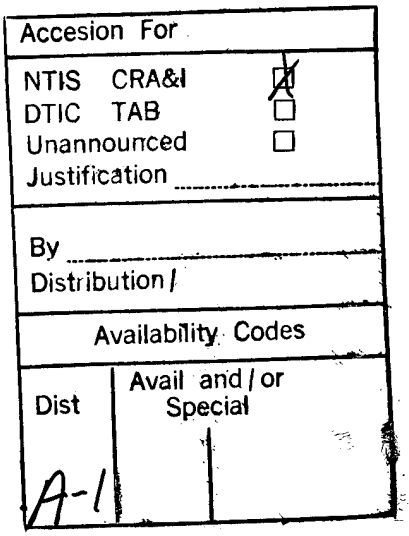




Prepared for
U.S. ARMY ENGINEER DISTRICT, ALASKA

## PREFACE

This report was prepared by Dr. Daniel E. Lawson, Research Physical Scientist, Geological Sciences Division, Susan R. Bigl, Research Physical Scientist, and John H. Bodette, Engineering Technician, Civil and Geotechnical Engineering Research Division, and Patricia Weyrick, Physical Science Technician, Snow and Ice Division, Research and Engineering Directorate, U.S. Army Cold Regions Research and Engineering Laboratory. Funding and support for this research was provided through the U.S. Army Engineer District, Alaska, Fort Richardson.

The authors thank William Gossweiler, Douglas Johnson, William Smith and Laurie Angell for helpful discussions, logistical support and assistance in the field, as well as their continuing support, and Dr. Charles Racine, Marianne Walsh and Charles Collins for numerous discussions on the Eagle River Flats project and their assistance in the field and laboratory. They also thank Lawrence Gatto and Lewis Hunter for their critical review of the draft manuscript of this report.

## CONTENTS



## ILLUSTRATIONS

Figure

Figure



## TABLES

Table

## EXECUTIVE SUMMARY

Eagle River Flats (ERF) is an estuarine salt marsh with a physical environment that is in a state of flux. Significant changes result from numerous forces, including a high tidal range, glacial river influences, large sediment influxes from two distinct sources, and a subarctic coastal climate. ERF is located within an active earthquake zone, further complicating process interactions and increasing the potential for rapid, but probably unpredictable, physical changes in the future. In addition, the U.S. Army has used ERF as an artillery range since the early 1940s. Ground explosions have caused physical changes to the terrain, hydrology and surface drainage.

Understanding the processes controlling the physical environment of Eagle River Flats is important because of our need to understand and remediate a problem of unusually high mortality rates in the migratory waterfowl that visit this area each spring and fall. Previous studies have shown that the high duck mortality is attributable to ingestion of elemental white phosphorus ($P_4$) particles (Racine et al. 1992a,b) that come from smoke-producing devices detonated either on or above the ground (Racine et al. 1992a). White phosphorus particles are now distributed within near-surface sediments of the ponds and marshes where dabbling ducks ingest it.

The inherent complexity of this dynamic environment makes it extremely difficult to predict what effects potential remedial measures for white phosphorus (WP) contamination will have on the physical system and, conversely, how the short- and long-term dynamics of the physical system will influence proposed remediations. Understanding both the system's response and the effects of such measures is critical to deciding what remedial technologies should be used.

Studies begun in 1992 initially appraised sedimentation and erosion rates in the C and Bread Truck pond areas. In 1993, we began to analyze the factors and processes controlling erosion, transport and sedimentation in this study area, while continuing and expanding our sedimentation and erosion measurements.

Tidal height fluctuations have been measured in concert with water level changes in two major gullies and in the Eagle River at the head of the Flats. These measurements are to define the timing and distribution of flood and ebb waters and to qualitatively assess the contribution of the Eagle River discharge to flooding in the study area. Suspended sediment concentrations were measured in the Eagle River, in gullies draining the Flats, and in Knik Arm to define the relative contribution of each source to pond and mudflat sedimentation. Salinity, temperature, dissolved oxygen, pH and turbidity were measured to assess the relative contributions of tidal or riverine water masses to flood and ebb cycle sedimentation and erosion. Physical parameters, including ground elevation, drainage pattern, channel gradients, flow velocity and gully dimensions, are necessary to calculate ebb drainage and sediment transport rates.

Sedimentation in the C and Bread Truck ponds complex is several millimeters per year on levees, 10–15 mm per year on the mudflats, and 20–40 mm per year in the ponds. Limited data on sediment concentrations in tidal flood waters of Knik Arm indicate that they exceed those of Eagle River discharge in August and September, suggesting that sediments are predominantly tidal (i.e., water masses of the Knik Arm). Sedimentation rates of 20 to 40 mm/year, if characteristic, are relatively high and would aid in infilling of ponds remediated by dredging or temporary draining.

Erosion and recession rates for the headwalls and lateral walls of gullies are also relatively high. Gullies are progressively extending into the mudflats toward the C and Bread Truck ponds complex. Headwalls and adjacent lateral walls receded at highly variable rates, ranging from 0.1–4.9 m during the summer of 1992, to 0.4–6.3 m during the winter of 1992–1993, and to 0.0–9.8 m during the summer of 1993. Large tidal floods in March, April, August and September of 1993 caused the greatest headwall recession. Two gully headwalls, one on the western side of Bread Truck Pond and the other near the pond complex between Bread Truck and C ponds, are advancing at rates sufficient to increase the drainage of those ponds within the next 10–15 years, if the

1993 rates persist. In the latter case, the headwall eroded to depths of about 1 m, extending the gully nearly 40 m into the mudflats.

Surveyed longitudinal profiles of gully thalwegs revealed gradients indicating that they will progressively grow into the mudflats by headwall erosion. Gradients near the Eagle River are relatively steep (0.01 to 0.02 m/m) in response to tidally controlled discharge variations in the river. Up-gully of the steep section, the lower reaches tend to range from about 0.003 to 0.007 m/m. With distance inland, channel gradients steepen to the base of the headwall. Headwalls have nearly vertical faces that vary from 1 to 2.5 m in height. Above them, drainage gradients across the mudflats into the ponds range from 0.001 to 0.004 m/m, being slightly lower in slope than within the gullies below the headwall. At several points in each gully, however, there are relatively sharp increases in gradient. These "knickpoints" are places where erosion is causing a progressive up-channel deepening of the gully thalweg, reducing the gradient in response to headwall erosion, and extending the gully farther into the mudflats.

Tidal flooding of the Bread Truck and C pond areas is enhanced by the discharge of Eagle River. Both the timing and height of maximum inundation are affected. Flood height can exceed the Anchorage datum by 0.5 m or more, the amount being highly variable, depending upon the volume of water in the Eagle River that enters ERF. A comparison of water level variations at the heads of two gullies in the Bread Truck–C pond areas and the tidal height variations in Knik Arm clearly showed such effects on tidal flood and ebb. In August, for example, seasonally high discharge from glacial meltwater in the Eagle River supplemented tidal flood heights and significantly increased the areas inundated. In September, precipitation in the Eagle River watershed of the Chugach Mountains also increased the height of two primary high tides, while the remaining tides were equivalent to Anchorage predictions.

The Eagle River provides access for tidal waters to inundate the innermost reaches of the Flats. Water level and stream flow as far inland as immediately upstream of the Flats proper can vary with tidal flood and ebb cycles. Our preliminary analyses suggest, however, that sedimentation in the lower two-thirds of ERF is tidally dominated, whereas the upper one-third appears to be river dominated. Aerial photographs from 1950, 1967 and 1993 suggest that the river has deposited its sediments upon entering ERF proper, forming an alluvial fan-like deposit, and distributing water flow in four radially spreading channels across the inner tidal flat. Remnants of mudflat and tidal pond terrain (e.g., Racine Island) are now mostly buried beneath material deposited during overbank flooding of the river in this area.

# Initial Analyses of Eagle River Flats Hydrology and Sedimentology, Fort Richardson, Alaska

DANIEL E. LAWSON, SUSAN R. BIGL, JOHN H. BODETTE AND PATRICIA WEYRICK

## INTRODUCTION

Eagle River Flats (ERF) is a 1000-ha tidal flat and salt marsh at the mouth of Eagle River on Knik Arm, near Anchorage, Alaska (Fig. 1). Previous work by CRREL has shown that an unusually high mortality of migratory waterfowl within ERF, particularly ducks, is attributable to ingestion of elemental white phosphorus ($P_4$) particles (Racine et al. 1992a,b). The primary source of white phosphorus particles is smoke-producing shells detonated during training on this artillery range, which has been active since the early 1940s (Racine et al. 1992a, 1993). White phosphorus (WP) particles are now present in near-surface sediments at numerous locations within ERF, including the pond and marsh bottoms where dabbling ducks ingest them during feeding.

Various remedial measures are being considered to control duck mortality from WP ingestion (Racine et al. 1993). Proposed remedies, which include dredging, draining ponds, placing geotex-

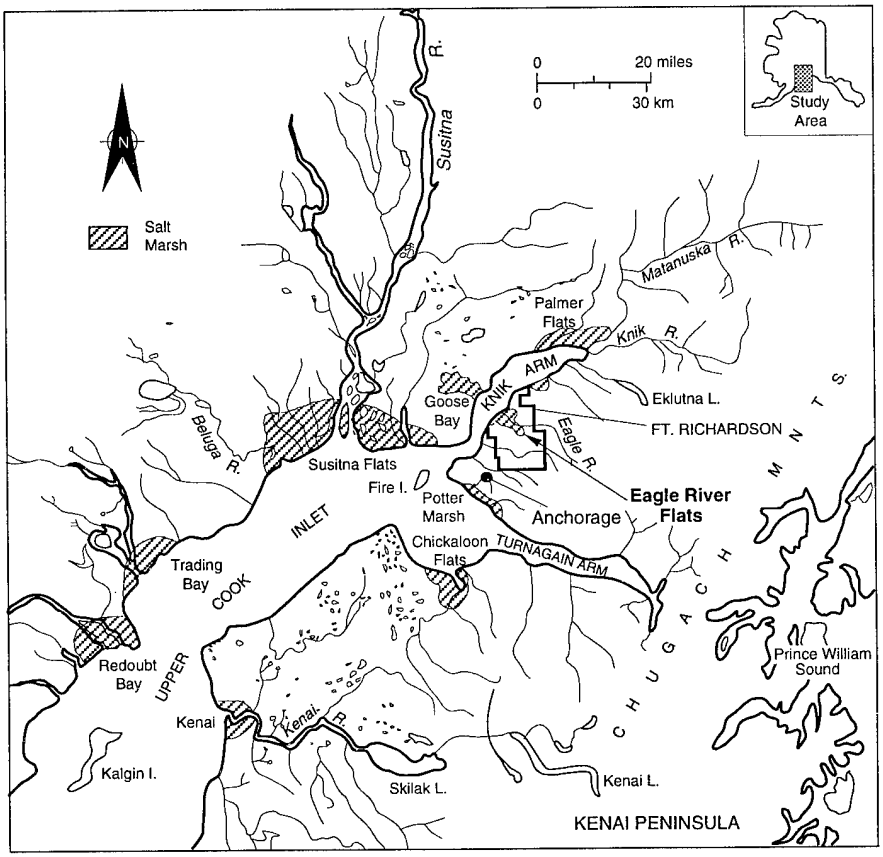


*Figure 1. Upper Cook Inlet region showing ERF and several other estuarine salt marshes (shaded areas).*

tiles or other ground covers, and enhancing sedimentation, will affect the physical ecosystem of ERF in ways that are largely unknown. Likewise, both the short- and long-term viability of these treatments will be influenced by the physical system, where the occurrence, intensity and interaction of the physical processes remain poorly understood. Baseline data are still required to define the sensitivity of the Flats to perturbations and to evaluate its responses to potential remedies. Restoration strategies will depend upon the methods chosen, but ultimately they must be compatible with the physical system.

In this report, we present the initial analysis of the physical system of Eagle River Flats, focusing on the interrelationships of the hydrological and sedimentological processes. Although preliminary, these initial results clearly demonstrate the complexity of the Flats' physical system and the need for further quantitative studies.

## GENERAL ENVIRONMENTAL CONDITIONS

Eagle River Flats is one of several estuarine tidal flats and salt marshes within the upper Cook Inlet region of south-central Alaska (Fig. 1). It lies at the mouth of Eagle River on the southeast side of Knik Arm and is about 2.75 km wide at the coast, narrowing inland. This region has a transitional maritime to continental climate, with generally moderate annual temperatures (daily mean 1.9°C; minimum mean –2.2°C) and precipitation (330 to 508 mm) (Evans et al. 1972).

A high tidal range with semi-diurnal fluctuations of 9.1 to 11 m and sediment-laden glacial discharges are critical factors affecting ERF hydrology and sedimentology (Lawson and Brockett 1993). Inundation results from both the tides in Knik Arm and the resultant overflow from the Eagle River as it meets the rising tide.

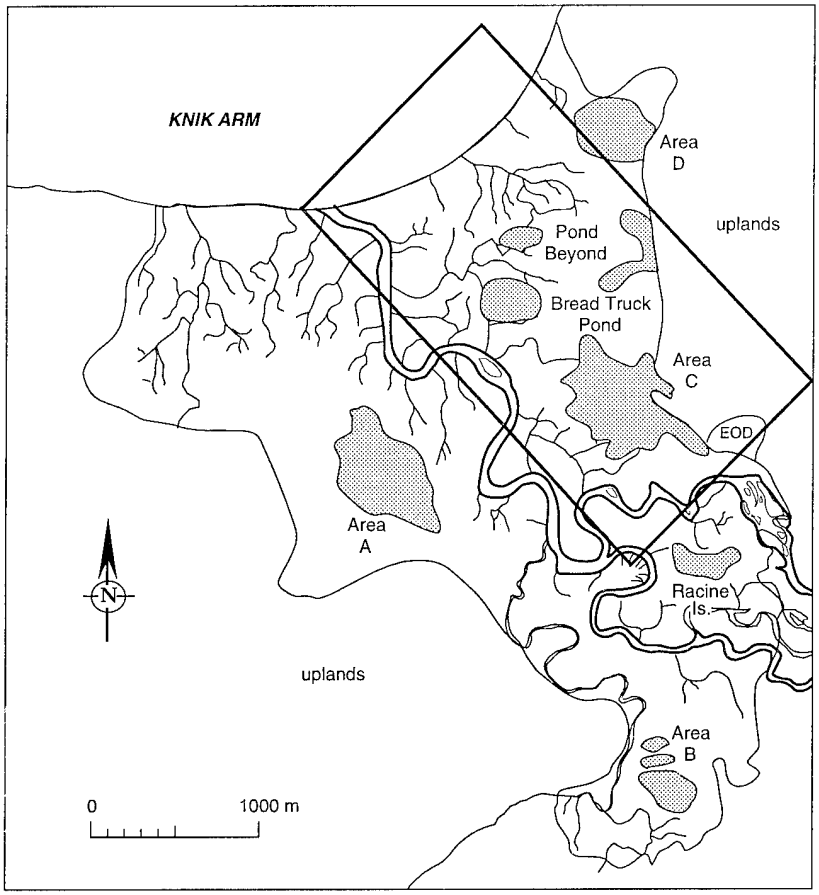


*Figure 2. General distribution of ponds (shaded areas) and the primary drainage system of gullies and vegetated channels within ERF. The primary study area was within the northeastern area marked by the rectangle.*

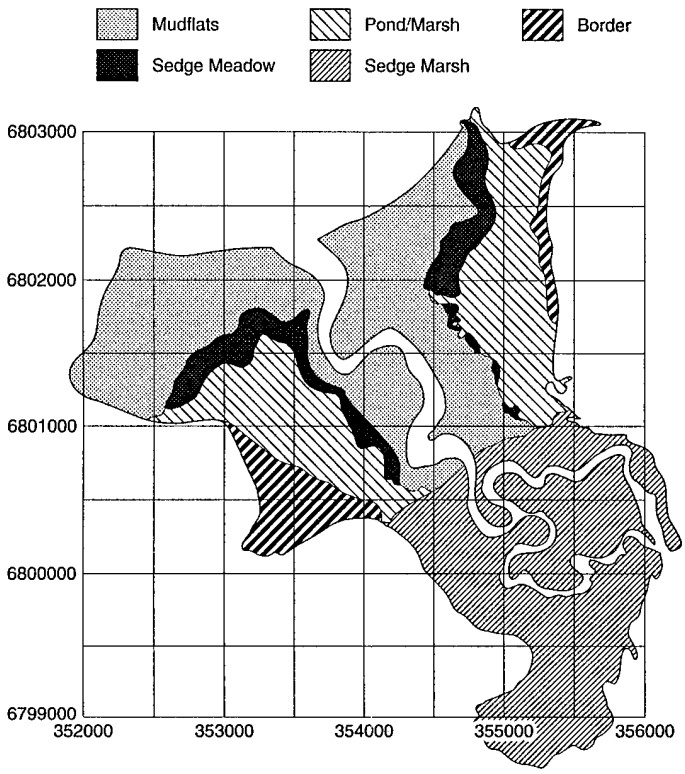


*Figure 3. Distribution of primary landform–vegetation units (from Racine et al. 1993).*

Eagle River drains a 497-km$^2$ basin in the Chugach Mountains, 13% of which is covered by glaciers. Average discharge was about 14.7 m$^3$/s from 1966 to 1981 (USGS 1981). Because of the Eagle River's glacial origin, its maximum and peak discharges take place during the primary melt season of July and August, with peak discharges exceeding 100 m$^3$/s when there are rainfall-induced floods during high melt periods.

The Eagle River cuts approximately through the middle of ERF. The area primarily drains laterally from ponds and marshes through vegetated channels and unvegetated gullies into the river channel (Fig. 2). About 20% of ERF is drained along the coast by gullies that discharge directly into Knik Arm. Its north and south boundaries are defined by uplands composed of glacial deposits covered by spruce and birch forests.

Sediments within both the Eagle River and the tidal waters of Knik Arm and Cook Inlet enter ERF, and both sources are derived mainly from glacier runoff. Massive quantities of silt- and clay-size particles are suspended within the numerous large rivers draining into the Inlet from glacierized basins in the Alaska Range, Chugach Mountains and Kenai Peninsula. These materials can remain suspended for extended periods and are transported into intertidal wetlands during tidal flooding. The Eagle River also transports glacially derived suspended sediment during the melt season. The quantity of suspended sediment entering ERF in transport by river and tidal waters is, however, unmeasured.

As with other estuarine salt marshes in Cook Inlet (e.g., Hanson 1951, Vince and Snow 1984, Rosenberg 1986), vegetation grows in zones that are commonly determined by elevation and related to the landforms of ERF (Fig. 3). This relationship is believed to be a function of flooding frequency, drainage capacity and sedimentation rates. Levees, mudflats, marshes and shallow ponds (to 50-cm depth) are arranged in a pattern that approximately parallels the Eagle River and coastline (Racine et al. 1992a). Freshwater ponds or shrub bogs lie along the upland bordering ERF.

## PREVIOUS STUDIES

The fundamental sedimentary and hydrological processes of subarctic and arctic tidal flats and salt marshes are not well understood; few quantitative analyses of these processes and the factors controlling their activity have been made.

The magnitude and variability in factors such as sediment supply, tidal regime, sea-level changes, local climate and storms, and wave and river activity can alter the relative importance and interaction of the physical processes in ways that remain poorly defined (e.g., Boon 1975, Frostick and McCave 1979, Carling 1981, Collins et al. 1987, Dionne 1988, Stoddart et al. 1989, Reed 1990, Dalrymple et al. 1992, Andrew and Cooper 1993). The role of glacial rivers and glacial–marine sediment discharges in tidal flat and salt marsh sedimentology have received only limited attention (Ovenshine et al. 1976a,b; McCann et al. 1981; Bartsch-Winkler and Ovenshine 1984). Neither the sediment fluxes nor the sediment budget of tidal flats and salt marshes are sufficiently defined to link their hydrology and sedimentology (e.g., Frostick and McCave 1979, Kohsiek et al. 1981).

Field studies and simulations of short-term sediment accumulation have suggested that process and morphology are related to elevation, and thus the annual frequency and depth of inundation and sediment supply, but that long-term rates may be more importantly controlled by the eustatic rise in sea level (e.g., Krone 1987; Allen 1990a,b; French 1991, 1993; French and Spencer 1993; McLaren et al. 1993). Spatial variations in the texture and composition of sediment deposited within tidal flats and salt marshes are also expected to relate to the hydrological processes of tidal channels and gullies, as well as tidal currents (e.g., Carling 1982, Allen 1992).

Sediment balance and the accretion and erosion of sediment in tidal flats and salt marshes have been estimated using short-term vertical sedimentation rates (e.g., Harrison and Bloom 1977, Richard 1978, Letzch and Frey 1980, Stoddart et al. 1989). Longer-term estimates have been made by dating subsurface horizons (e.g., Hubbard and Stebbings 1968, Allen and Rae 1988) and creating radionuclide profiles (e.g., Bloom 1984, Keene 1971, Kearney and Ward 1986). Both estimates, however, may be misleading owing to compaction after deposition in the former case and time-dependent accretion rates in the latter (French 1993).

## STUDY AREA AND METHODS

This study focused on the central area of ERF, east of the Eagle River, extending from west of the EOD pad to the outer coast (Fig. 2). The morphological terrain units in this area are

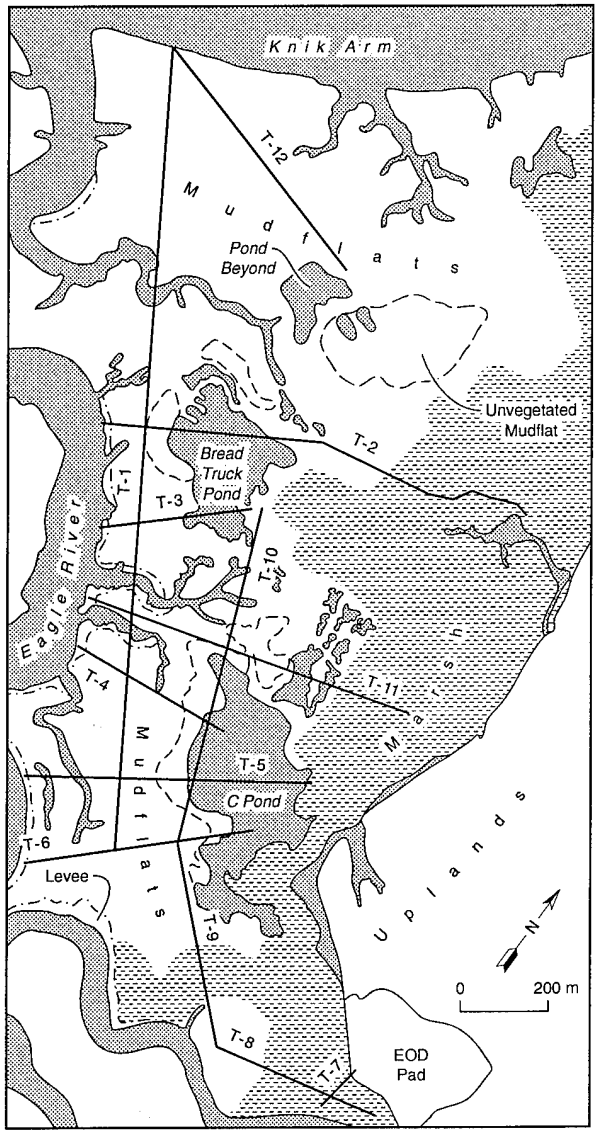


*a. Surveyed transects within areas from the EOD pad north to the Knik Arm coast.*

*Figure 4. Location of sedimentation study sites.*

levees, gullies, upper vegetated mudflats and lower unvegetated mudflats adjacent to ponds and marshes.

Eleven transects across the representative morphologic units of the study area were established in May 1992, with one additional added in June 1993 (Fig. 4a) (Lawson and Brockett 1993). Surveying established ground surface elevations on each transect relative to local benchmarks and the UTM grid. Grab samples of the surface sediment (to 5 cm depth) were taken at each survey point (Fig. 4b) for analysis of the grain size distribution using standard sieving

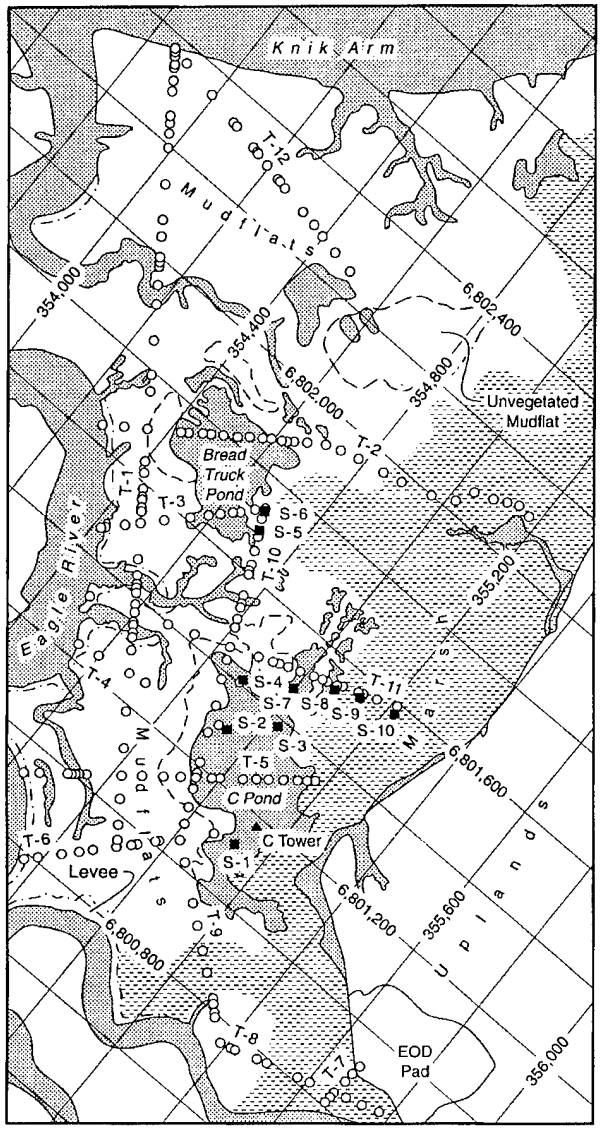


*b. Surveyed locations of surface grab samples (open circles) on 12 transects east of Eagle River. Open circles also mark the locations of sedimentation stakes. Filled squares are locations of sedimentation stations (S-no.).*

*Figure 4 (cont'd).*

and hydrometer techniques. These data will be used to delineate textural trends and evaluate the relative importance of sediment sources.

**Sedimentation and erosion**

Sedimentation rates within tidal flats are difficult to measure accurately. Within ponds and marshes, for example, only a slight disturbance of the water column is needed to resuspend the fine-grained bottom sediments. If these sediments are caught in sediment traps, erroneously high depositional rates would be measured. We

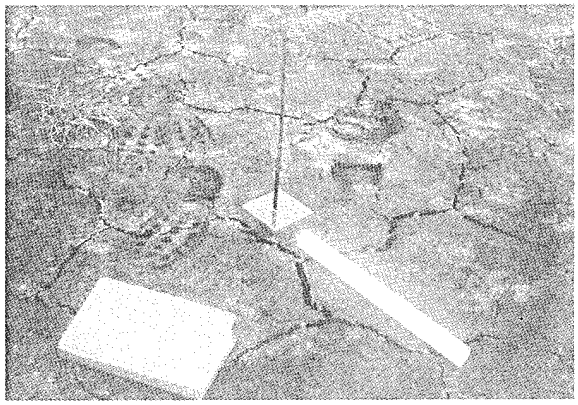

*Figure 5. Sedimentation stakes. The plate slides freely on the rod. Wire flags mark an area of painted ground that is now covered with sediment.*

therefore used several methods to measure the primary rates of sedimentation and related erosion, and the secondary rates of resedimentation that result from resuspension of pond bottom materials by various processes. Depositional and erosional rates were also measured in the mudflats, levees and gullies. The various samplers described subsequently were installed during 24–28 May 1992, with several sets of measurements taken between then and 28 September 1993.

"Sedimentation stakes" were used to measure erosion and deposition at points along the surveyed transects (Fig. 5). These stakes consist of a rod and a square, rigid plate (about 7 $cm^2$) that slides freely on the rod. Erosion depth is defined by the increase in distance between the top of the rod and the top of the plate, as measured periodically to the nearest 0.5 mm. The amount of accretion is the thickness of sediment deposited on the plate surface. The difference between these two readings defines the net sedimentation (or erosion) rate. We measured these rates in July, August and September 1992 and in May and September 1993, following the monthly period of tidal flooding. A similar stake system was used previously in Turnagain Arm (Ovenshine et al. 1976a,b).

We also monitored the amount of accretion at transect survey points by spraying an area (30× 30 cm) on the ground surface with pavement marking paint and locating the corners of this area with wire survey flags. Net accumulated sediment is measured by cutting and removing a 2-×2-in. (5-×5-cm) block of sediment with a putty knife (Fig. 6). The thickness of sediment above the paint layer is then measured to the nearest 0.5

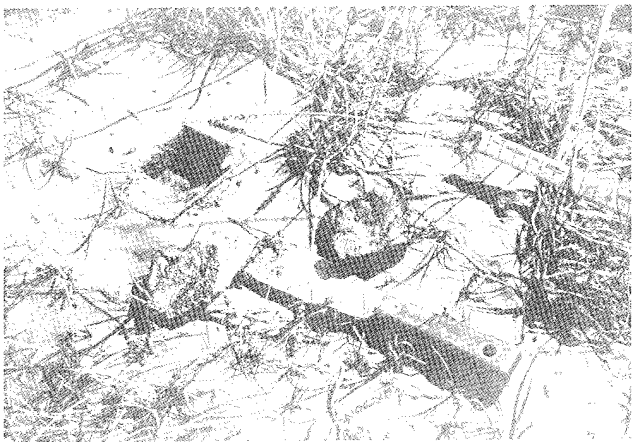

*Figure 6. Paint layer within block of sediment as measured to define sedimentation rates.*

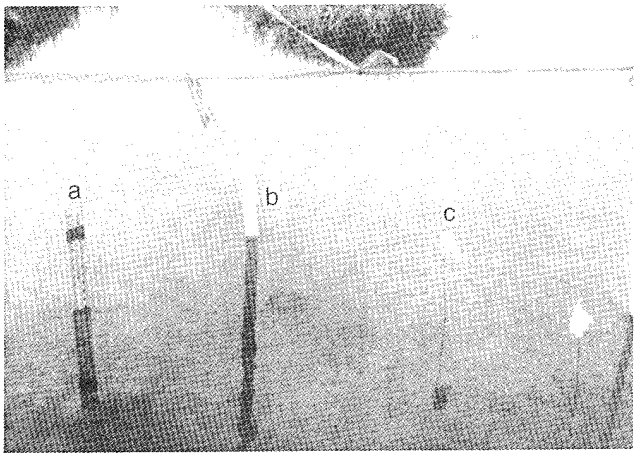


*Figure 7. Sedimentation station in a pond site. A meter stake (a), cup sampler (b) and plate sampler (c) are shown in position. The plate sampler is located between the two survey flags.*

mm with a millimeter scale. Paint was applied at certain sites in June 1992, and others in mid-August 1992. In contrast to sedimentation stakes, which are broken or removed by various processes during winter, the wire flags and the persistence of buried paint horizons suggests this method may provide a continuous record of net sedimentation rates.

Sedimentation rates in ponds were also measured at 10 sites following tidal inundations in June, August and September 1992 and May and September 1993 (Fig. 4). We expected these rates to be extremely low and possibly to be affected by resuspension of bottom sediments during the process of obtaining data. We, therefore, used three methods at each site initially, but have found two to be relatively reliable.

Gross deposition is measured in a sediment trap consisting of a 4-in.-diameter (10.2-cm-diameter) PVC "cup" glued to one end of a short length of 2-in.-diameter (5-cm-diameter) PVC pipe. The pipe was inserted into the pond until the bottom of the cup was in contact with the bed (b on Fig. 7). Sediments held within the cup include new sediment brought into the ponds by tidal inundation and river currents, and materials resuspended by wind waves, dabbling ducks or other mechanisms. The quantity of accumulated sediment is measured to the nearest 0.5 mm by inserting a millimeter rule into the sediments at three places. After measurement, the sediment in the cup is cleared away.

We measured the net sedimentation rate in ponds using a thin, rigid plastic plate of about 30 cm square that is pushed gently into the pond bottom until it is flush with the surface. The corners of the plate are secured by aluminum tent pegs (c on Fig. 7). Sediment in suspension settles onto this plate, but this sediment can also be reworked and resuspended by wind or other mechanisms, thereby delineating a net rate. In addition, by measuring the sediment thickness at three random locations, the plate's dimension provides some measure of the spatial variability in sedimentation or erosion rates. Plates are covered by sediment, and later by aquatic vegetation, within one to two weeks or less of placement; this cover negated the possible effects of their smooth surfaces on their sediment trapping efficiency.

Initially in 1992, a stake with a millimeter-

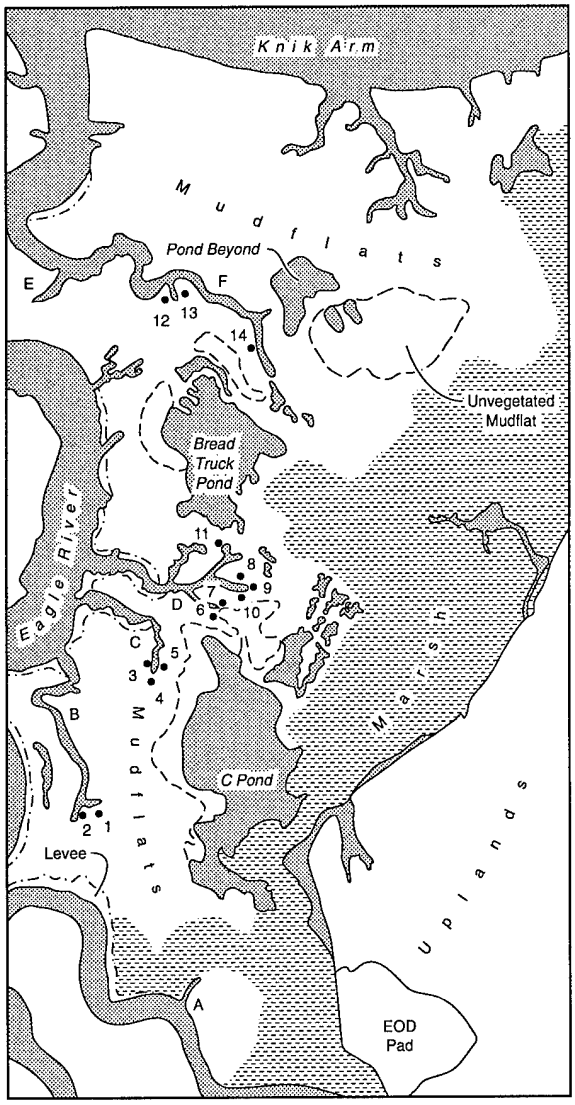


*Figure 8. Location of gully headwall erosion study sites.*

*Figure 9. Headwall erosion study site. The line of stakes approximately parallels the gully crest. The hub stake is to the right of center behind the stake line.*

graduated scale on its face was inserted into the pond bottom, and the height of the pond bottom and the water column were measured to provide a second measure of the net sedimentation rate (a on Fig. 7). Any wind waves or water surface glare on sunny days, however, commonly made this a difficult measurement to obtain. In addition, aquatic vegetation on the bed commonly covered the base of the scale. For these reasons, only water level measurements are now recorded.

**Gully erosion and recession**

Gullies* draining the ponds and mudflats are actively extending inland by headwall and lateral wall erosion and recession. We established 14 sites to evaluate retreat rates (Fig. 8); 11 sites were established in June 1992, 3 in June 1993. At each site, stakes were driven into the ground along a straight line at known distances from one another and from the crest of the gully (Fig. 9). A "hub" stake was set at a known distance from this stake line. The distance between the hub and the crest of the gully scarp was measured across the top of each line stake in succession with a tape measure. The position of the gully scarp was identified with a plumb bob suspended from the tape measure. Flagged wire stakes were then placed at each point of measurement along the headwall.

Measurements were repeated in September 1992, June 1993 and September 1993 after tidal inundation. On the basis of repeated measurements at points without any retreat (as indicated by the continuing presence of wire flags), we consider these measurements reproducible at ±2–5 cm. The accuracy, however, is limited by how well the crest of the gully scarp can be defined, the shape of which is highly irregular, and therefore accuracy is probably limited to ±10 cm.

The elevations of the bed along the length of several gullies were surveyed, beginning at or near the Eagle River and continuing into the ponds (Fig. 10). These gradients were calculated from these data for characteristic reaches in each gully. Gradients were incorporated into estimates of gully discharge and current velocity at surveyed cross sections during maximum or bankfull ebb.

* The terms gully and drainage are used interchangably.

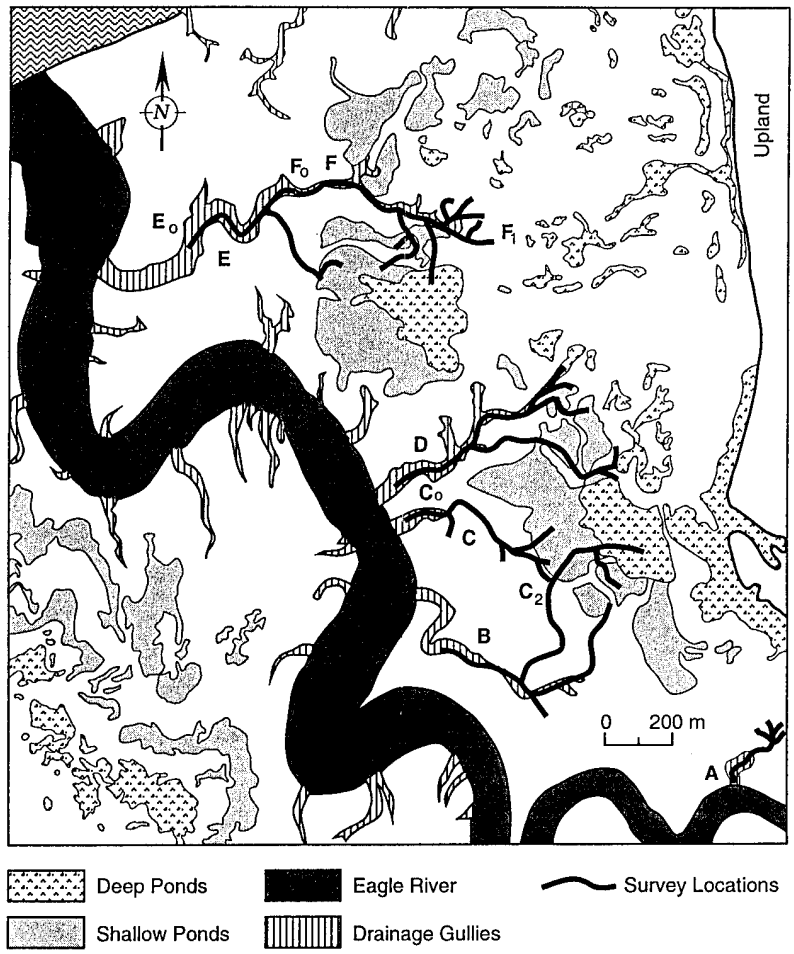


*Figure 10. Location of surveyed longitudinal cross sections of gullies.*

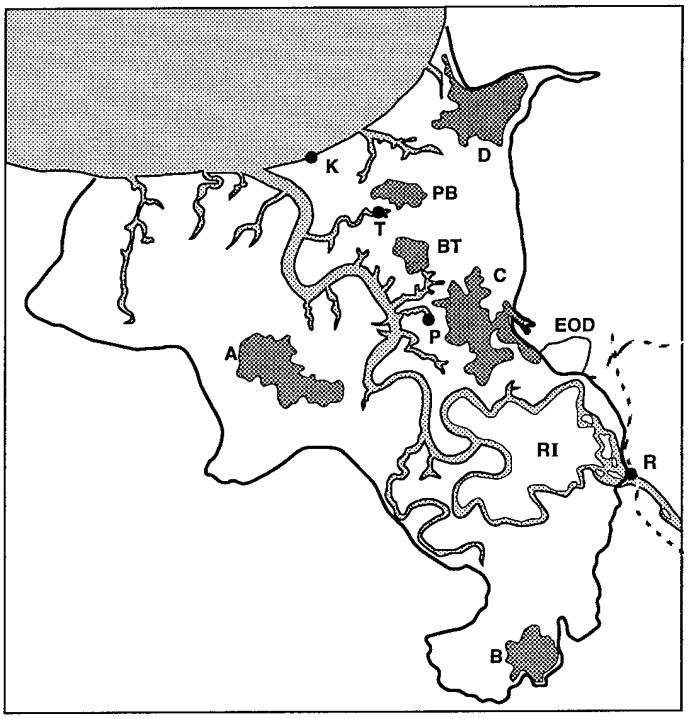


Instrumentation sites:
K – Knik Arm
P – Parachute drainage
R – Eagle River
T – Bread Truck drainage

Other site abbreviations:
BT – Bread Truck pond
PB – Pond Beyond
RI – Racine Island

Ponded areas labeled A through D

*Figure 11. Locations of instrumentation recording water quality parameters and water depths.*

**Table 1. Specifications of water quality parameter sensors.**

| *Instrument type* | *Sensor* | *Accuracy* | *Resolution* |
|---|---|---|---|
| Hydrolab | Temperature | ±0.15°C | 0.01°C |
| ($H_2O$ multiprobe) | pH | ± 0.2 units | 0.01 units |
| | Specific conductance | | |
| | Fresh water | ±0.0015 to 0.1 mS/cm* | 0.001 mS/cm |
| | Salt water | ±0.15 to 1.0 mS/cm* | 0.01 mS/cm |
| | Salinity | ±0.2 ppt | 0.1 ppt |
| | Dissolved oxygen | ±0.2 ppm | 0.01 ppm |
| | Redox | ±20 mV | 1 mV |
| | Depth | ±0.45 m water | 0.1 m water |
| CRREL thermistor | Temperature | ±0.02°C | 0.01°C |
| Druck (PDCR 950) | Pressure (water depth) | ±0.008 m water | 0.001 m water |
| OBS–3 | Turbidity 5 V = 2000 FTU | ±100 mV | 1 mV |
| Seagauge Wave/Tide | Pressure (water depth) | ±0.003 m water | 0.0015 m water |
| (model SBE 26–03) | Temperature | ±0.02°C | 0.01°C |
| Seacat CTD | Pressure (water depth) | ±0.75 m water | 0.045 m water |
| (model SBE 19–03) | Temperature | ±0.01°C | 0.001°C |
| | Conductivity | ±0.001 S/m | 0.0001 S/m |
| | OBS [5V = 2000 FTU] | ±100 mV | 3 mV |

* Depends on which of three auto-adjusting ranges is employed.

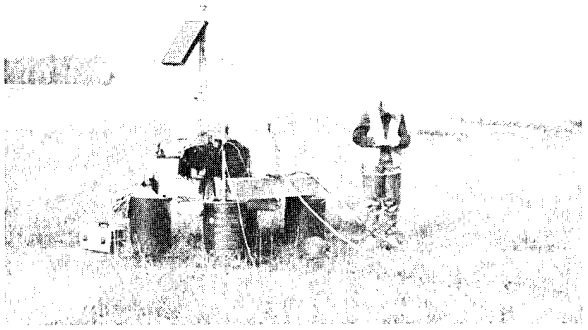

*a. Platform.*

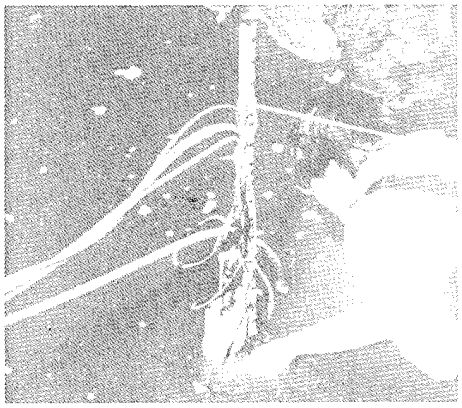

*b. Sensor detail.*

*Figure 12. Platform and instrumentation measuring discharge characteristics at the Bread Truck gully location.*

**Water quality parameters**

Water quality characteristics were analyzed during the August and September 1993 flood and ebb cycles at two gully sites—one in a gully draining C Pond (called Parachute gully or drainage) and one in a gully draining the Bread Truck Pond area. The same measurements were made in the Eagle River, just downstream of the Route Bravo access road bridge (Fig. 11).

A Campbell CR10 datalogger was used to record data from a variety of sensors. A Hydrolab Model H20 Multiprobe Transmitter provided data on a suite of parameters related to WP particle and sediment transport: temperature, pH, salinity, dissolved oxygen, redox and water depth (Table 1). We also used a Druck pressure transducer to measure water level variations to ±8 mm, an individually calibrated thermistor to measure temperatures to ±0.02°C, and a D&A OBS–3 optical backscatter sensor to measure turbidity.

Data loggers and other instrumentation were positioned on a floating platform next to gullies, while the various sensors were mounted on stakes set into the small plunge pools at their heads (Fig. 12). Sensors were placed in the plunge pools to keep them wet at all times.

Each platform was constructed of a 4-×4-ft (1.2-×1.2-m) plywood deck mounted on a 2-×6-in. (5-×15-cm) frame. Large metal eyehooks were screwed into the frame on each corner (Fig 12a);

5-ft (1.5-m) sections of 0.75-in. (2-cm) diameter steel pipe were mounted vertically in large cans filled with concrete, and the eyehooks mounted on the platform's wood frame were lowered over them. Foam filled the inner space of the deck framework and provided flotation so that the platform could move vertically up or down the steel pipes during tidal inundation and ebb. The platforms allowed us to establish monitoring stations without setting stakes or foundations in the ordinance-bearing mudflat sediments and, at the same time, keep the data loggers and related devices dry even under the highest flood levels.

An ISCO Model 3700 water sampler, also mounted on each platform, obtained 500-mL water samples at specific intervals through the flood and ebb cycle. The Total Suspended Sediment concentration (TSS) of each sample was analyzed using standard vacuum techniques with 45-mm glass microfiber filters. The TSS data were later used to calibrate the D&A Optical Backscatter Sensor (OBS) turbidity readings for sediment concentrations measured at each site.

Water quality data were recorded from mid-August to the end of September using 2-minute sampling intervals at the gully sites and 10-minute intervals at the river site. A Seabird SBE19 Profiler or CTD (Conductivity–Temperature–Depth) profiler was moored at the coast in Knik Arm from mid- to late September to measure salinity, temperature, depth and turbidity during several of the tidal cycles (Fig. 11). At the same location, a Seabird SBE26 Wave and Tide Gauge measured tidal height variations and water temperature from mid-August to late September (Table 1). ISCO water samples were acquired at $^1/_2$-hour intervals through the flood and ebb cycles of August, but this was changed in September to a 10-minute interval about peak tide. Water samples were also taken by hand from Knik Arm at the wave and tide gauge recorder during the September inundation cycle.

## PROCESS OBSERVATIONS

The activity and relative importance of erosional and depositional processes depend upon a number of factors, including those that are external to the immediate Flats environment. External factors include tidal forces, glacially derived runoff and sediment, climate, and tectonic and earthquake activity. In addition, a slowly rising sea level and isostatic rebound following occupation of the region by glaciers that retreated about 12,000 years ago may be affecting processes as well.

The glacial sources for the Eagle River modify the discharge seasonally, mainly in response to variations in climate, and daily, mainly in response to diurnal changes in ablation and meltwater runoff. Maximum discharge occurs during and following the spring runoff of snowmelt, but may remain high throughout the summer, depending upon meteorological factors affecting meltwater production on the glacier surface (e.g., Röthlisberger and Lang 1987, Lawson 1993). Rapid, hourly fluctuations in discharge may result from heavy rain in the river's watershed.

The glacially derived sediment within runoff from the watershed also varies seasonally and annually; within ERF, this component mainly affects the amount of sediment in suspension. Sediment in suspended transport from the Eagle River is one potential source of material deposited within the ponds and mudflats.

Tidal flood waters are another major source of suspended sediment. These sediments are likewise of glacial origin, being derived from glacierized watersheds feeding major rivers that enter Knik Arm and Cook Inlet, including the Susitna, Knik and Matanuska rivers. It is not known whether the seasonal and annual variability of sediment discharge from these glacial rivers is evident within the tidal waters of Knik Arm. Limited measurements of Knik Arm in November 1993 and March 1994 indicated that sediment is in suspension through the winter, but in smaller quantities than during the summer. The continued presence of suspended sediment during winter is important, as it would then be the most important if not the only source of sediment for deposition during that time. The Eagle River, as with other glacial rivers, transports an insignificant amount of material in suspension during the fall through the early spring when glacial discharge is limited to groundwater sources (e.g., Lawson 1993).

The interaction and combination of tidal and river sources of water and sediment control the amount of material available for deposition in ERF, and may also affect the locations and rates of erosion. The amount of sediment within flood waters is a primary factor determining their capacity to erode and transport additional sediments during ebb.

A preliminary analysis of aerial photographs of ERF suggests that sedimentation of the landward third of the area (southern one-third) is

dominated by the Eagle River. Landform types and distribution differ here, being mainly levees and vegetated marsh floodplains. These riverine landforms overlie and cover older marshes, a part of which is apparently exposed in the center of Racine Island (Fig. 13c). In the northern two-thirds of ERF, landforms are similar to tidal flats near river mouths elsewhere in this region (e.g., Ovenshine et al. 1976b).

Historical aerial photographs and ground observations also indicate that ERF is physically changing over both short- and long-time scales. Large-scale changes resulting from riverine processes over the last 40 years include abandonment of a primary channel within the southern part of the Flats, and channel migration of various amounts from near the Route Bravo bridge north to the river mouth at Knik Arm.

Aerial photographs from 1950, 1967 and 1993 reveal that the primary river channel (of three) was abandoned sometime between 1950 and 1967 (Fig. 13). By 1967, two channels diverged from Eagle River north of the Route Bravo bridge, the primary avenue of discharge now appearing to be the eastern course. Our initial review of these photographs does not reveal the cause of this change; however, it is clearly important to understanding the hydrology and sedimentology of the Flats.

The two primary channels entering the Flats today are partially braided and have a divergent pattern characteristic of an alluvial fan (Fig. 13c). Both suggest that the channel gradient significantly decreases near the bridge, leading to a reduction in carrying capacity, deposition of sediments in transport, and a fundamental change in the channel configuration (e.g., Leopold et al. 1964). In addition, the 1993 color infrared image shows a well-defined change in texture and color where these channels merge into a single meandering channel (Fig. 13c). This textural change may indicate a physical change, such as in elevation, or in the grain size and mineralogy of the substrate materials. The predominant types of vegetation reflect these physical differences and thus the apparent change from river dominated to tidally dominated physical processes.

Both the tributary channel and the meandering main channel progressively deepen downstream, essentially being incised over 5 m during low tide. Near-vertical scarps and evidence of recent slumping indicate that the river banks are actively eroding. A qualitative assessment of the 1950, 1967 and 1993 aerial photography suggests that, historically, banks have receded several tens of meters at some locations.

Significant changes in the relatively tight meander loops in the lower section of the river have taken place over the last 40 years. Landforms, such as meander scars and abandoned point bars, are common along the length of the active channel and are especially evident on photographs of the southern reaches of the Flats (Fig. 13c). These landforms result from changes in the channel location over time. Channel changes are a natural progression resulting from the erosion and recession of the outer banks of meander bends, deposition of sediments as point bars within the inner parts of each bend, and a general downstream migration of the channel (e.g., Allen 1982). At some locations, a breaching of tight meander loops causes their abandonment (Fig. 13c).

Erosion associated with channel changes remobilizes bank sediments, which may be transported either downstream or upstream, depending upon the capacity of the river and tidal forces. In the idealized river model, they would move to the next point bar and be redeposited. Redeposition will also be controlled by tidal and river processes and by the materials' fine grain size, and therefore they may also be redeposited within the ponds and mudflats, as well as within Knik Arm.

Gullies have also progressively lengthened and deepened during the last 40 years, in some cases extending over an estimated 200 to 300 m. A significant extension of gullies toward the ponds and marshes is particularly evident on photographs covering the period of 1967–1993 (Fig. 13b and c), but the amount of recession cannot yet be quantified. Recession is in response to erosion during ebb flow from the ponds and mudflats into the gullies (Table 2). Erosion measurements in 1992 indicated that this recession is continuing at variable rates of up to 5 to 10 m per year (Lawson and Brockett 1993).

The cause of gully expansion is unclear, but it may be a response to external forces such as earthquake activity, including the 1964 Alaskan earthquake when this area subsided about 0.6 m (Small and Wharton 1969), the eustatic rise in sea level, or large-scale river channel changes caused by flooding. Further quantitative analyses of historical aerial photographs and sedimentological analyses of deposits within the alluvial landforms are required to determine


*a. 1950.*

*Figure 13. Aerial photographs of ERF.*


*b. 1967.*

*Figure 13 (cont'd).*


*c. 1993.*

*Figure 13 (cont'd). Aerial photographs of ERF.*

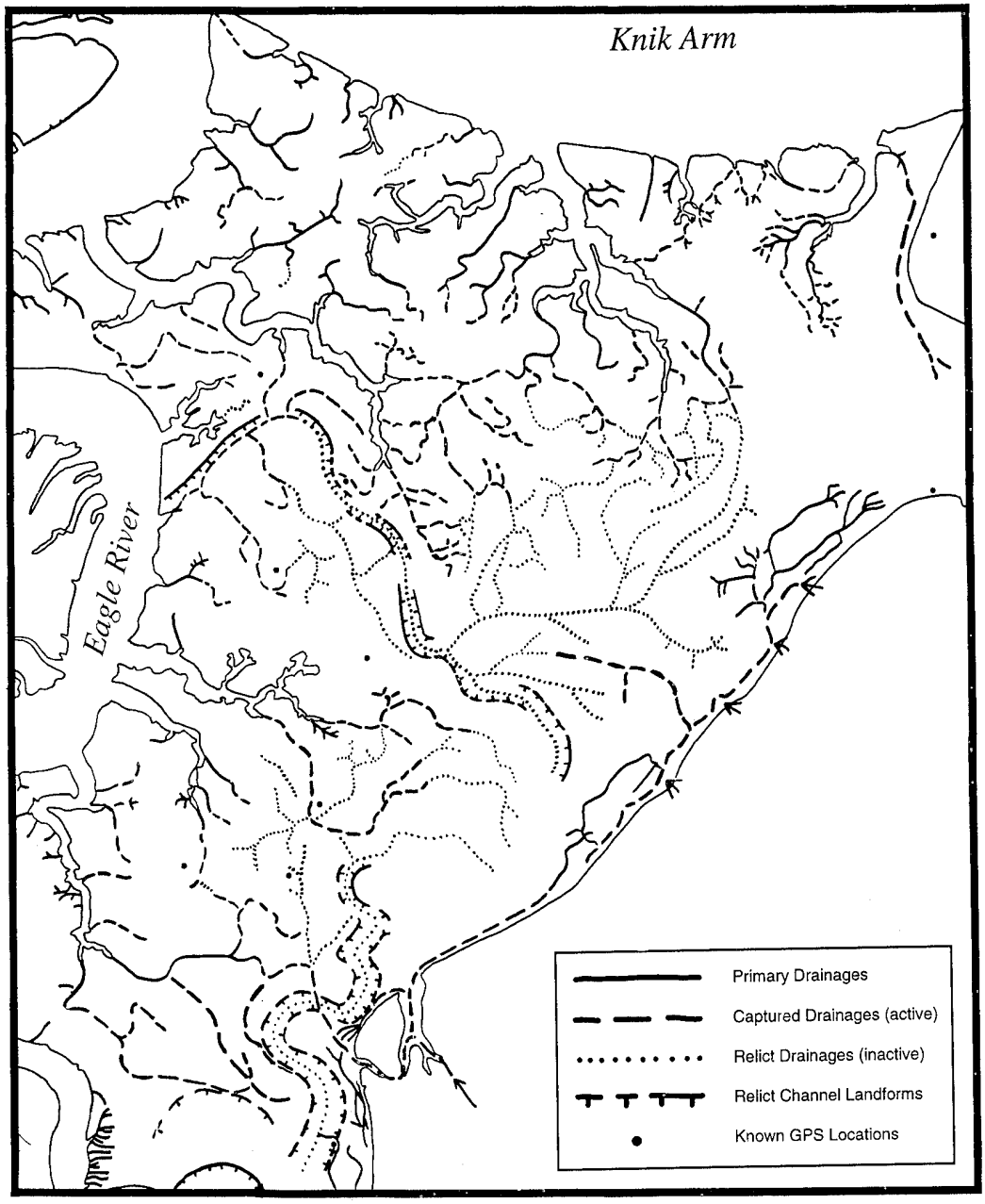


*Figure 14. Drainage pattern analysis of 1993 aerial photograph in the study area east of Eagle River.*

**Table 2. Summer erosional processes.**

| *Morphological unit* | *Processes* | |
|---|---|---|
| Ponds | Currents<br>—wind<br>—tidal<br>Wind waves<br>Wind currents<br>Ducks and other bottom-feeding organisms | Tidal currents<br>Debris impacts (e.g., logs) |
| Gullies | Currents<br>—tidal<br>—runoff<br>Overland flow<br>—sheet<br>—rill<br>Wind waves | Groundwater<br>—piping<br>—sapping<br>Slope mechanisms<br>—slump<br>—block collapse<br>—sediment flow |
| Mudflats | Currents<br>—wind<br>—tidal<br>Overland flow<br>—sheet<br>—rill | Wind waves<br>Debris impacts (e.g., logs)<br>Rain drop impact |
| Marshes | Currents (rare) | |
| Levees | Currents<br>—tidal<br>—river | Debris impacts<br>Wind waves |

whether the gullies are expanding in response to such external forces.

Tributary channels with a dendritic pattern feed water into the gullies (Fig. 14). These shallow, vegetated channels cross the mudflats and head in the ponds. A second set of channels that is intercepted by the active tributary system is also common (Fig. 14). These channels, however, unconformably cross other landforms, including ponds (such as C and Bread Truck) where they lie below the water surface. Their pattern is irregular and unrelated to the dendritic channel and gully system. These secondary channels are probably relict drainage and indicate significant changes to the drainage in the past. The causes of such changes are unknown, but may be related to larger scale forces such as flood-induced channel migration or earthquake-induced subsidence.

## GLACIER RUNOFF AND SEDIMENT YIELD

Runoff from the Eagle River is characteristic of a watershed occupied partly by glaciers. Glaciers cover about 13% of the watershed area, yet it takes only a few percent glacier cover to significantly modify the runoff and sediment yield of a drainage basin (e.g., Lawson 1993). Glaciers modify peak discharges, the timing and maximum and minimum volume of hourly, daily and seasonal discharges, the lag between precipitation and the resultant increase in runoff, and long-term trends in annual discharge of the basin (e.g., Gurnell and Clark 1987, Lawson 1993). Water quality parameters, including suspended solids, show similar, but not directly related, variations with time.

The USGS recorded discharge from the Eagle River between 1966 and 1981 (USGS 1981). During this period, daily discharge averaged 14.7 $m^3/s$. The maximum mean discharge during the height of the glacial melt season (July–August) averaged 42.5 $m^3/s$, with peaks ranging from about 65 to 76 $m^3/s$. Rain-induced floods during peak glacial runoff exceeded 105 $m^3/s$. Unfortunately, a new station to record discharge of the Eagle River could not be installed in 1993, and we therefore do not have current hydrologic records for the Eagle River.

We were, however, able to establish instrumentation in mid-August to measure basic water quality parameters, suspended sediment concentrations and water level changes through September. These data show diurnal variations in water height, conductivity and temperature typical of a glacially fed river (Fig. 15) (e.g., Lawson 1993). Sediment concentrations were generally low from 25 August to 20 September, ranging from 23 to 275 mg/L and decreasing steadily through September. Additional water quality and sediment transport data will be acquired during 1994.

## TIDAL HYDROLOGY AND INUNDATION

Erosional, transport and depositional processes are complexly related to tide height, Eagle River discharge, and the length of time of inundation. Although sufficiently high tides can flood all of ERF, lower high tides may be supplemented by the river's discharge and flood more area to a greater depth than the predicted tide height indicates. During spring snowmelt runoff, precipitation-induced flooding or other high discharge events, tidal waters moving up the channel block the flow of the river water, causing it to slow and pool, and eventually can reverse flow within the Flats proper. Some overflow of the tidal water by fresh river water may also take place. The flooded area is increased and runoff during ebb is prolonged. Similarly, increased flooding can result from storm-driven waters moving into the Flats from Knik Arm and Cook Inlet.

Pond sedimentation results mainly from set-

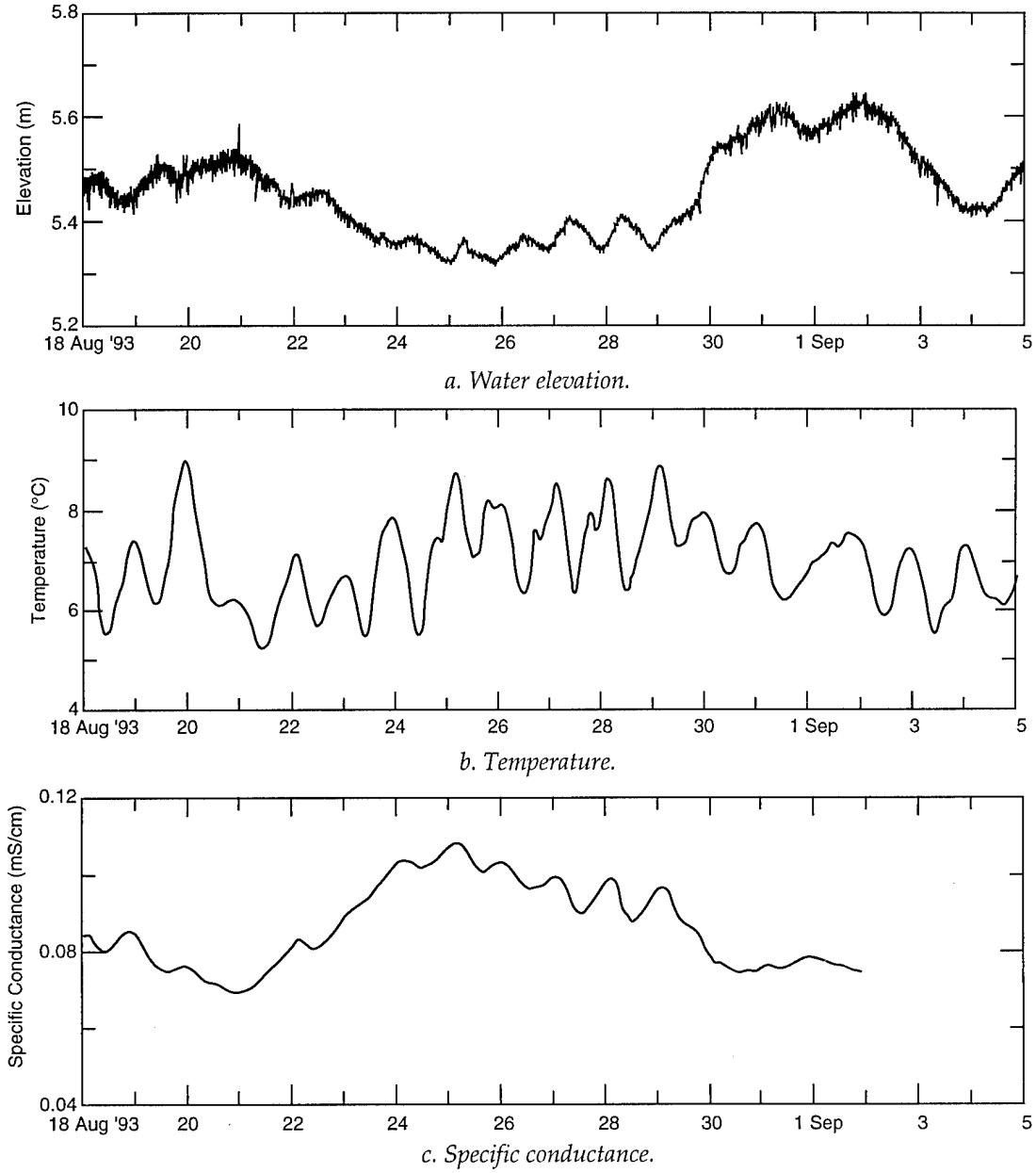


*a. Water elevation.*

*b. Temperature.*

*c. Specific conductance.*

*Figure 15. Water parameter data from Eagle River site just downstream of Route Bravo bridge.*

**Table 3. Summer depositional processes.**

| *Morphological unit* | *Processes* |
|---|---|
| Ponds | Suspension sedimentation<br>—settling-out<br>—vegetation trapping |
| Gullies | Suspension sedimentation<br>—settling-out<br>Bedload deposition<br>Sediment flows<br>Slumping |
| Mudflats | Suspension sedimentation<br>—settling-out<br>—vegetation trapping |
| Marshes | Suspension sedimentation<br>—vegetation trapping |
| Levees | Suspension sedimentation<br>—settling-out<br>—vegetation trapping |

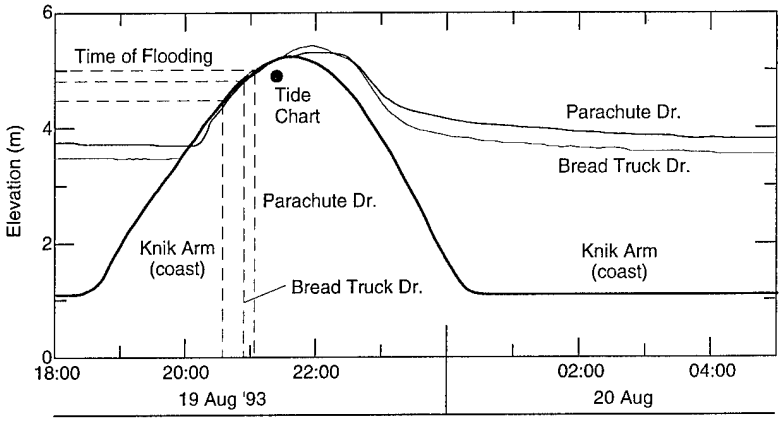


*Figure 16. Water elevation at three sites during the 19 August evening flood event. The base level shown on the Knik Arm plot is equal to atmospheric pressure measured when the sensor is exposed in air.*

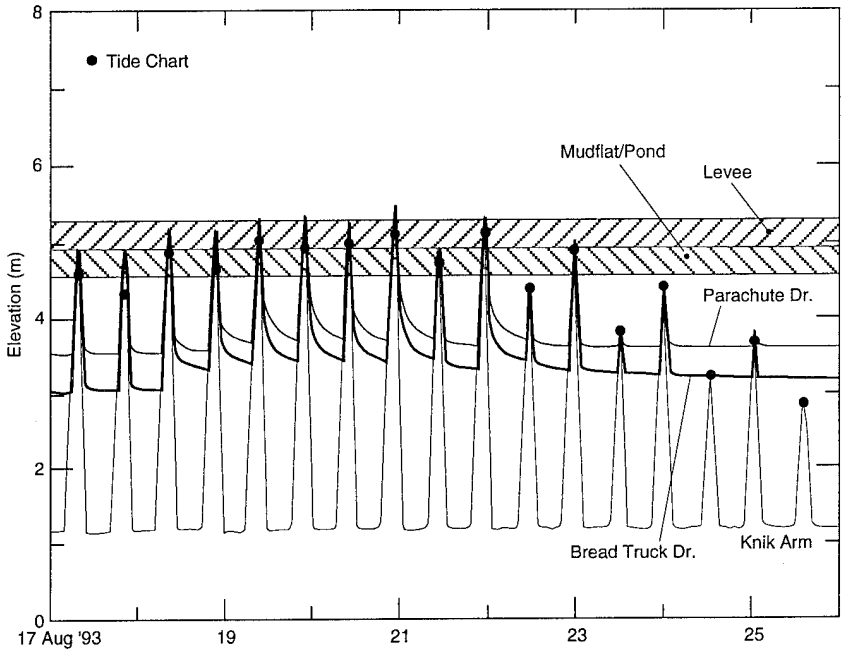


*a. August.*

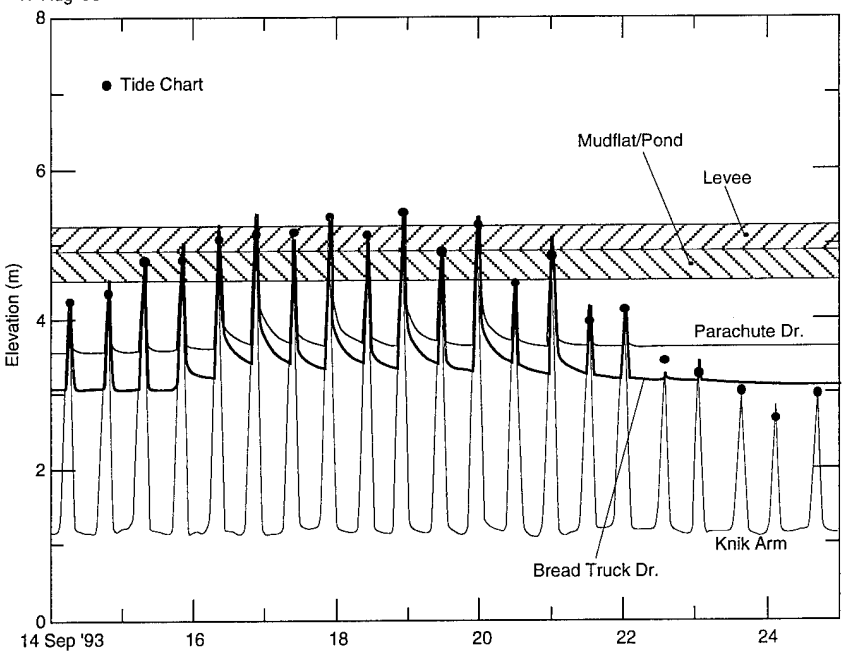


*Figure 17. Water elevations at three sites during a period of flooding cycles. Knik Arm represents the tidal cycle external to ERF proper. In August, Parachute and Bread Truck data show peak heights greater than predicted due to various factors including high river flow, but little augmentation over predicted heights in September.*

*b. September.*

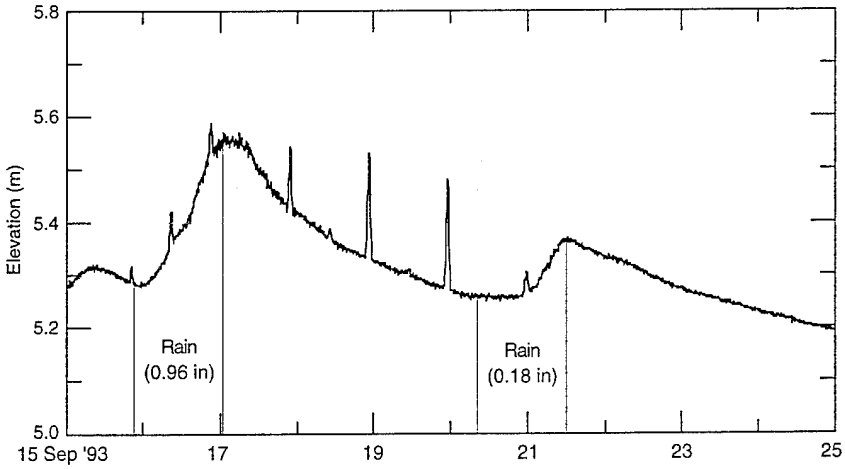


*Figure 18. Elevation of waters in Eagle River during September flooding cycles. Rainfall in the watershed affected elevation twice during the September tidal cycles.*

tling-out of sediment suspended in the water column (Table 3) and, presumably, sediments are deposited mainly following slack high tide. Thus, the longer the period of inundation, the greater the time for sediment in suspension to be deposited. In addition, the mixing and exchange of flood waters with the original pond and marsh waters increases the amount of sediment suspended in the ponds and marshes, and provides the primary source of newly deposited materials.

The timing of flooding is a function of both the elevation of the levees and mudflats surrounding the gullies, and of the distance of the gully headwall from the coast. Water moving down the river can also alter the timing of flooding inland from the coast, depending upon its volume relative to the volume of tidal waters. A quantitative relationship for these factors is not yet developed, and thus the relative duration of inundation per tidal flooding cannot be predicted.

Water level measurements at the river and gully sites (Fig. 11) verified our visual observations that the flood cycle normally results in a progressive rise in the river channel and gully water levels before a gradual flooding of the tidal flats takes place. This progression is illustrated by water height changes at the three sites during a tidal inundation in August (Fig. 16). Flooding begins first within the coastal mudflats on Knik Arm, while water is progressively moving inland up the Eagle River channel and the tributary gullies before it spills onto the inner mudflats first at the Bread Truck gully and then at Parachute gully. Water levels decline first in the coastal zone, actually while tidal flood waters are still moving up Otter Creek and into the southwestern corner of the Flats.

Water levels were also greater than predicted for the Anchorage datum from 17–22 August, showing primarily the effects of a high glacial meltwater discharge in the Eagle River (Fig. 17a). Precipitation and wind were not factors during this time.

Water heights measured at these same sites during tidal flooding in August and September illustrate the seasonal shift from higher to lower discharge as melting of glacial river sources is reduced (Fig. 17b). Flood heights generally exceed the tide chart predictions for Anchorage in August, until the discharge decreased around 22 August. In September, flood heights generally match predicted tide levels; whenever they exceeded those levels, river discharge had been increased by rainfall in the Eagle River watershed (Fig. 18).

## WATER QUALITY PARAMETERS AND TIDAL FLATS HYDROLOGY

Water quality during tidal influx and efflux is critical to understanding the interplay of tidal flood waters and river discharge and to examining their role in the erosion, transport and deposition of sediment within the Flats. Water quality parameters were only measured during two summer months (August and September), so that we can only speculate on the overall role of tidal and riverine water sources. The relative importance of these parameters as a data source can, however, be illustrated by examining variations in selected parameters during a flood and ebb cycle at the Bread Truck Pond gully on 18 August 1993, at the Bread Truck and Parachute gully sites on 19–20 August, and at both sites on 18–19 September.

Data during the flood and ebb cycle of 18 August show the basic relationships of water quality parameters to inundation (Fig. 19). As

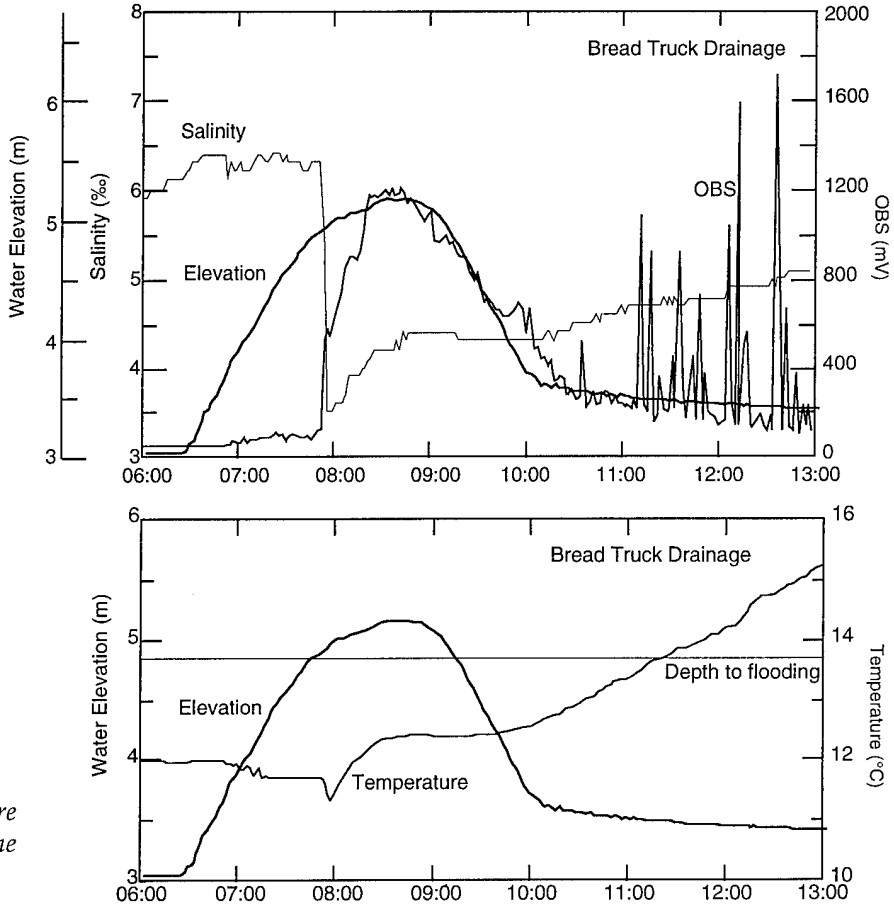


*a. Water elevation, salinity and optical backscatter measurement.*

*b. Water elevation, temperature and depth to flooding of the mudflats.*

*Figure 19. Variation of water quality parameters, Bread Truck drainage site, 18 August.*

the flood tide progresses into ERF, it moves up the Eagle River, backing river waters up each gully, and causing them to spill onto the mudflats. The water level rises initially at a steady rate, but rapidly decreases as the area being flooded increases when the water crests the gully headwall and spills into the vegetated drainageway and onto the mudflats above it. Water temperature, salinity and turbidity change in the headwater pool in which the sensors are submerged as its water is exchanged with the more saline tidal flood waters. Just before the headwater pool attains conditions that reflect the character of Knik Arm waters, parameters may fluctuate rapidly while the mixing front of the two water masses passes.

During ebb, the drop in water level is slower than the rise during flooding, indicating temporary storage of tidal waters within the Flats. The stored water may include river influx and possibly may involve temporary storage in the sediments as groundwater. The transition from more saline tidal flood waters to fresh or pond-dominated waters therefore takes place more gradually. In part, the more gradual change in temperature and salinity, for example, results from mixing and homogenization in the ponds and mudflats.

The sharp, transient rises in turbidity are, however, related to some other process. They may be caused by vegetation or fish covering the optic sensor, but are most likely actual increases in turbidity from sediment in transport. The increased turbidity may be caused by scour of the gully headwall or lateral walls, or perhaps sudden bank failures, causing a rapid, but local, increase in the amount of sediment suspended in the water column. Until ebb waters are completely contained in the gully channel during the latter stages of runoff, water may flow into the gullies at numerous locations along their lengths.

Data from the heads of the Bread Truck and Parachute drainages during a flood and ebb cycle on 20–21 August of a predicted high tide of 10.0 m and on 18–19 September of a predicted

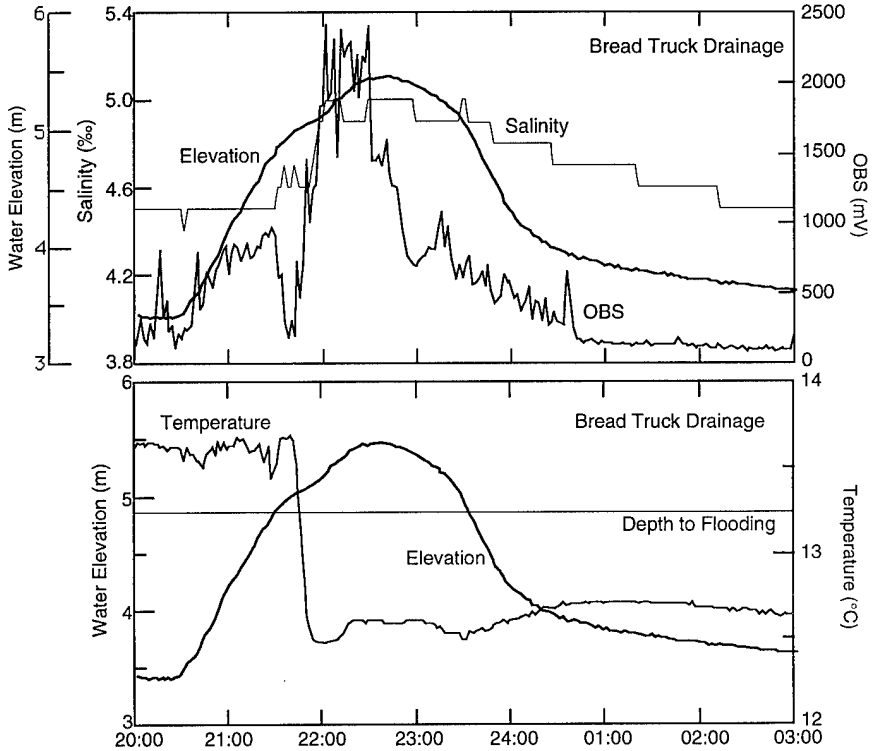


*a. Bread Truck drainage.*

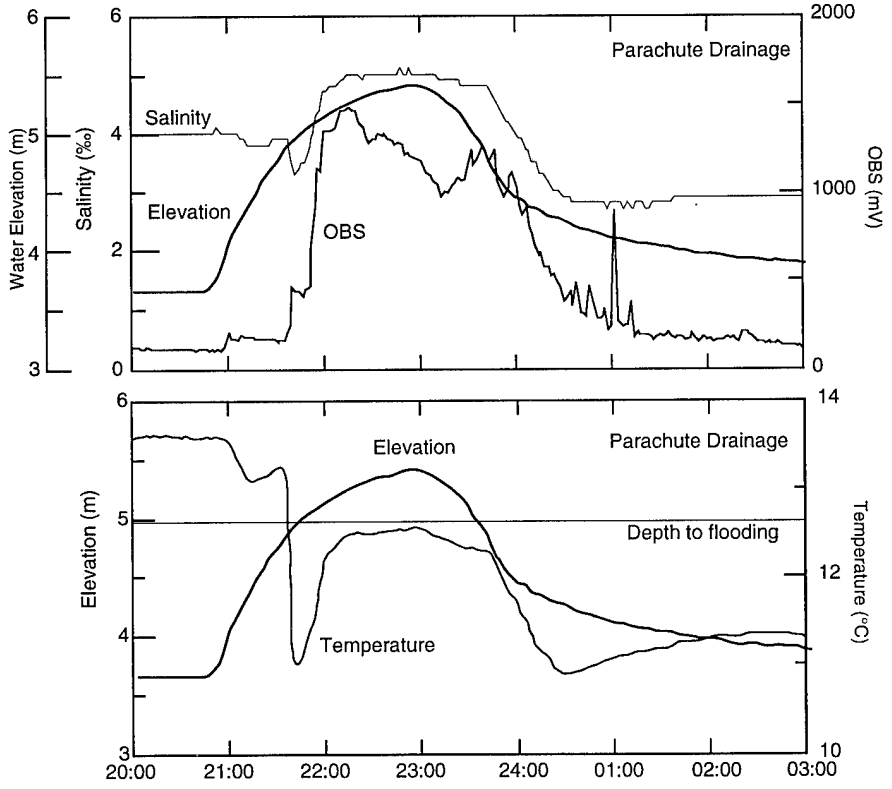


*b. Parachute drainage.*

*Figure 20. Variation of water quality parameters, 20–21 August.*

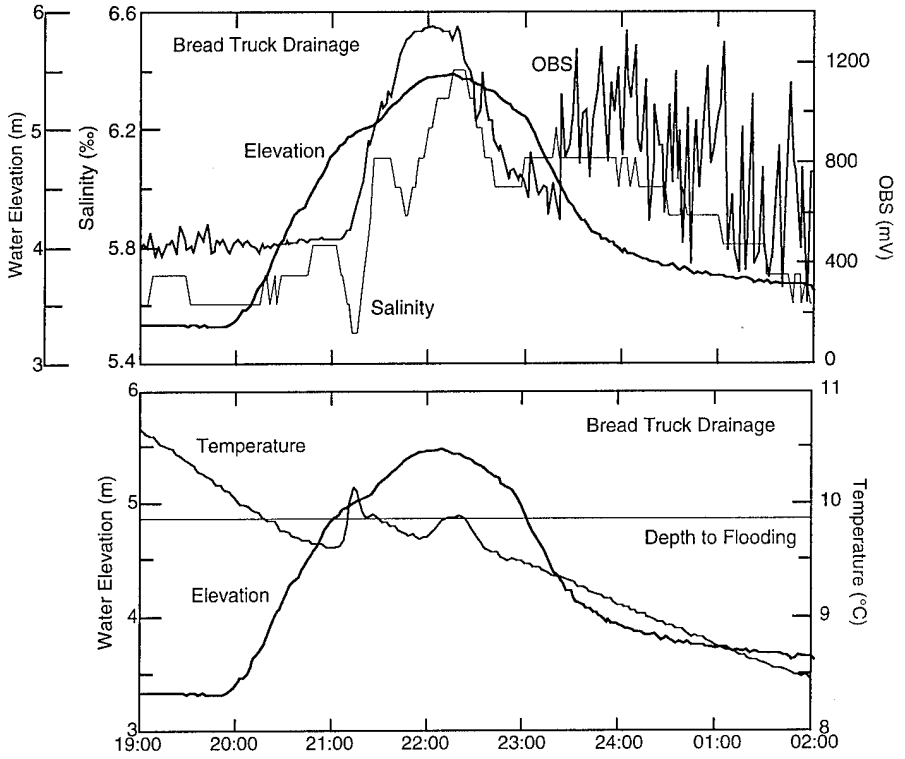


*a. Bread Truck drainage.*

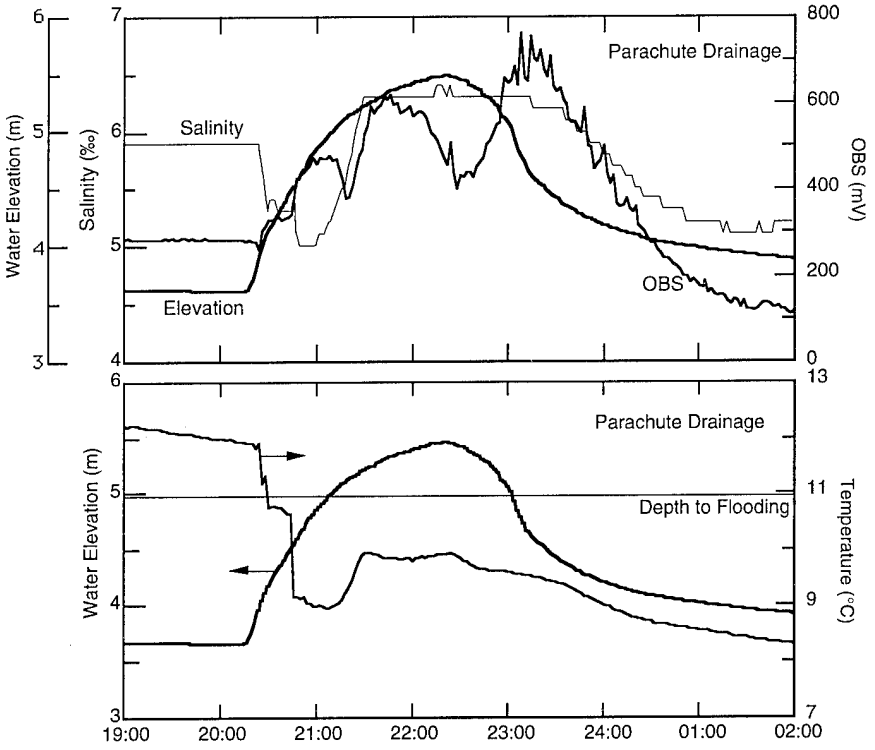


*b. Parachute drainage.*

*Figure 21. Variation of water quality parameters, 18–19 September.*

**Table 4. Temperature and salinity of Eagle River and Knik Arm.**

| | 20 August | | 18 September | |
|---|---|---|---|---|
| Site | Temperature (°C) | Salinity (ppt) | Temperature (°C) | Salinity (ppt) |
| Eagle River | 6.0 | 0 | 4.0 | 0 |
| Knik Arm | 12.9 | — | 10.3 | 6.8 |

high tide of 10.33 m illustrate several important aspects of tidal flats hydrology (Fig. 20 and 21).

As described for 18 August at the Bread Truck site, the water level on 20–21 August rises rapidly as flooding begins, but slows as water spills into the vegetated drainageway above the gully headwall and floods the mudflats. Coincident with this rise, water temperature, salinity and turbidity change but in different ways at the Bread Truck than at the Parachute site.

At the Bread Truck gully site, where the flooding threshold is lower, water temperature shows little variation until the approximate time when water height is sufficient to overflow the gully. Temperature then rapidly declines to near that of water in Knik Arm, signaling the arrival of tidal flood waters (Table 4). Small temperature variations (tenths of a degree Celsius) during the remainder of the tidal cycle may result from local mixing of tidal and fresher water masses. Coincident with the temperature drop, turbidity increases sharply and remains high through flooding; however, just after this rise, OBS values decrease sharply, perhaps reflecting an initial override of fresher water by the intruding more saline tidal floodwaters.

As ebb takes place, turbidity values drop rapidly within about 30 minutes, indicating either that waters inundating the Flats have lost their suspended sediment through deposition in ponds and mudflats, or that the mixing of river and tidal water masses has diluted the concentration of solids. With time, the turbidity continues to decrease as water elevation declines; both sediment concentration and salinity decrease to levels present before the flood.

At the Parachute gully site, the drop in temperature accompanying the initial encroachment of flood waters is greater than at Bread Truck. This reduction is believed to be attributable to a higher proportion of river water in the first flood waters rising to the gully sensors because of the more inland location of the gully mouth. Salinity, turbidity and temperature sharply increase as the tidally dominated water mass subsequently fills the gully (Table 4).

As ebb occurs, the decrease in turbidity takes place more gradually than at the Bread Truck site until the water elevation drops below bank height. Then it decreases rapidly, as does temperature and salinity, to levels less than Knik Arm, suggesting that river water is a larger component of the ebb discharge at the Parachuate site.

In contrast, the 18–19 September tidal event is characterized by lower suspended sediment concentrations, higher salinities and lower water temperatures (Fig. 21). Several other important aspects are also evident. At Bread Truck, the temperature does not decrease rapidly as the tidal waters rise. An initially lower temperature within the plunge pool during September than in August may account for a temperature similar to that of water in Knik Arm (Table 4). Both turbidity and salinity increase rapidly, however, as flooding takes place. The rapid drop in salinity just before peak flood level may indicate incomplete mixing of Knik Arm and Eagle River waters within the flood. During ebb, water temperature and salinity gradually decline as the freshwater component becomes more important, but the turbidity values exhibit a series of rapid fluctuations that nearly equal those during peak flood.

The Parachute gully record has a more gradual and sustained fall in turbidity beginning at about the same time as at the Bread Truck site. The source of this difference from Bread Truck is unknown, but we speculate that the sustained values at Parachute represent discharge of sediment transported from within the Flats. The pulses of suspended sediment in the water column may result from local erosion, failure and collapse of the gully walls. But this argument is less convincing for the Bread Truck site; the highly erratic peaks are more likely caused by vegetation that caught on the probe.

Of further note are the significantly higher salinities in the Parachute flood and ebb waters in September than in August. These values probably represent the seasonally reduced contribution of Eagle River water to flooding of the Flats. Similarly, turbidity values at both sites were less than in August and correlate with reduced concentrations of suspended sediment in both the river and Knik Arm. This reduction is also a response to the seasonal drop in sediment discharge from the glacierized basins that flow into the Eagle River and the rivers entering Knik Arm.

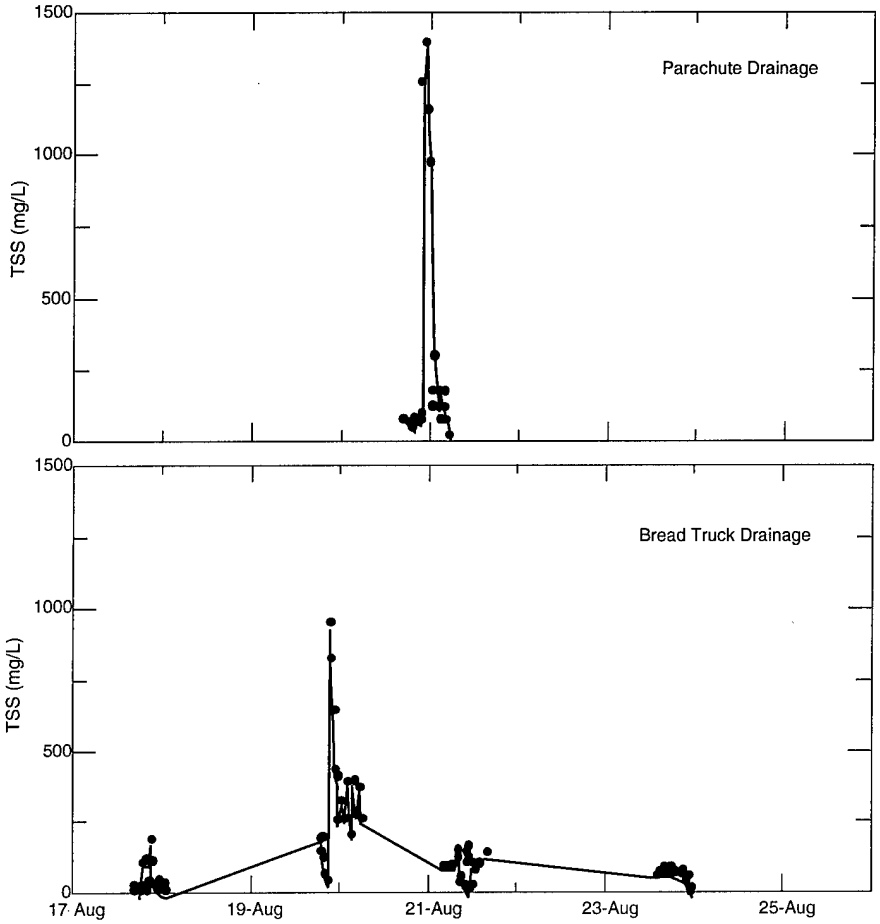


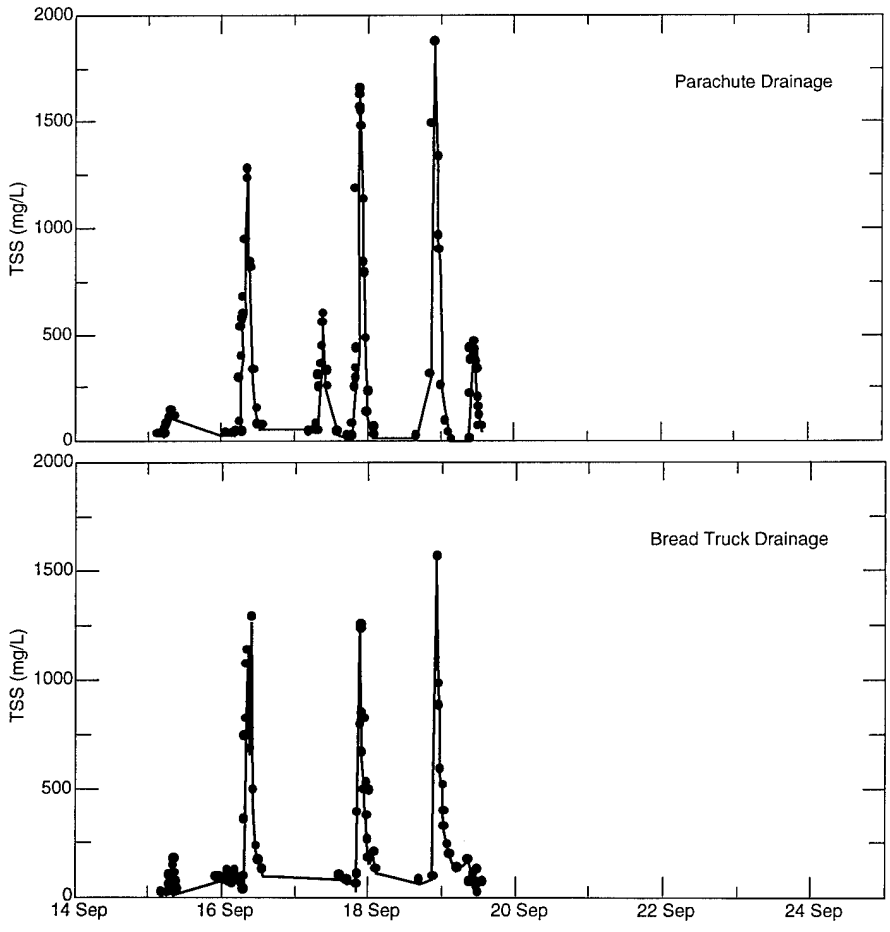


*Figure 22. Total suspended sediment (TSS) concentrations measured at gully sites during August and September flooding cycles.*

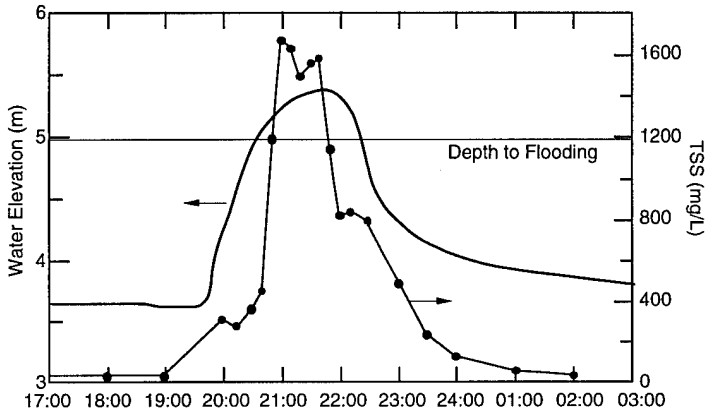


*Figure 23. Total suspended sediment concentrations and water elevations at Parachute drainage, 17–18 September.*

## SEDIMENT TRANSPORT

Sediments are deposited within ponds and mudflats mainly through settling-out from waters flooding ERF (Table 3). New materials are in suspended transport by river and tidal flood waters, while a second source is sediment eroded and remobilized from the pond bottoms and mudflats by wind currents, bottom-feeding waterfowl and other mechanisms. River currents may also erode sediment from riverbanks; gullies likewise can be eroded by flood or ebb currents. Total Suspended Sediment (TSS) in discrete samples and the continuous recording of turbidity by an Optical Backscatter Sensor (OBS) provide data on suspended sediment transport and the relative importance of sediment sources.

Samples for TSS analysis were obtained during the August and September flooding cycles at the Parachute and Bread Truck gully sites (Fig. 22). During the August cycle, water samples were taken every half hour over 12 hours running from low tide to low tide. Relatively low values were recorded at the Bread Truck drainage in three of four recorded cycles; the fourth event produced a peak value of 1000 mg/L (Fig. 22b). In one cycle recorded at Parachute drainage, the samples captured a peak of 1500 mg/L (Fig. 22a).

This sampling scheme did not sufficiently represent the variability in suspended sediment concentration over time and therefore the sampling interval was altered in September. Samples were then acquired every 10 minutes, beginning near the predicted peak high tide at Anchorage and continuing through the initial phase of the ebb. The time interval was progressively lengthened to a half hour and then one hour during the latter stages of ebb, as well as for several hours prior to high tide.

In the first sampled event of 15 September, flood levels were barely high enough to spill onto the mudflats above the gullies and low TSS peaks were recorded at both sites (170 mg/L) (Fig. 22). Subsequently, the morning tide of 16 September flooded most of the Flats up to about 0.2 m depth; both Parachute and Bread Truck had similar TSS peaks of approximately 1250 mg/L. Flooding cycles sampled on 17, 18 and 19 September were characterized by deeper inundation (about 0.4 m) and higher peak TSS values. TSS peak values in the Parachute drainage were 1700 and 1900 mg/L, exceeding the Bread Truck values by 300 mg/L. In general, low suspended sediment concentrations characterized the rising tide while flood waters moved into each gully. A sharp rise in TSS occurred as the rising flood waters from Knik Arm began to spill onto the mudflat. Suspended sediment concentrations gradually declined only after ebb began (Fig. 23).

OBS turbidity levels peak during flooding of the gully sites in August, generally ranging from 1300 to 1500 mV (500 to 600 FTU) at Parachute gully and 1200 to 2300 mV (480 to 920 FTU) in the Break Truck gully (Fig. 24a and b). In both cases, the OBS values indicate that sediment concentrations progreasively increase as tidal waters enter and flood each site, gradually falling at a slower rate as ebb takes place and gully drainage becomes well established. In September both sites had lower ranges in turbidity (about 700 to 1300 mV [280 to 520 FTU] at Bread Truck and about 800 mV [320 FTU] at Parachute [Fig. 24b, c and d]). The OBS records for a SBE19 CTD temporarily established at the tide gauge

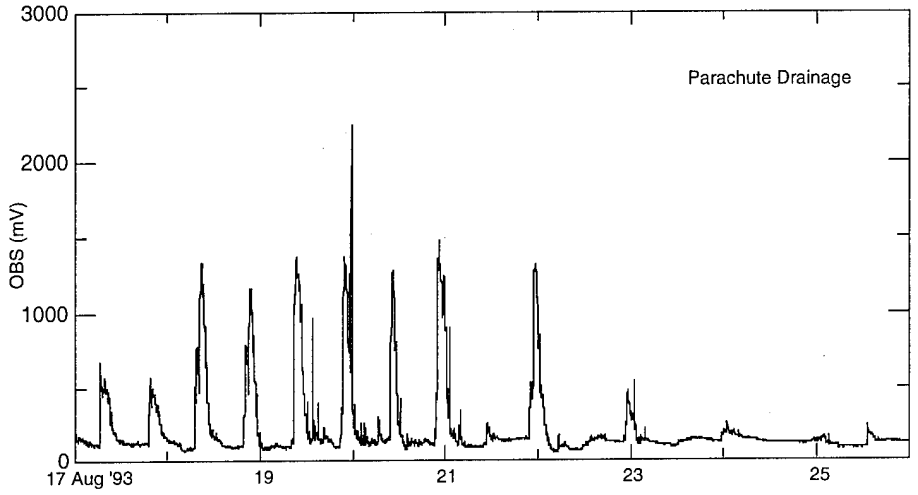


a.

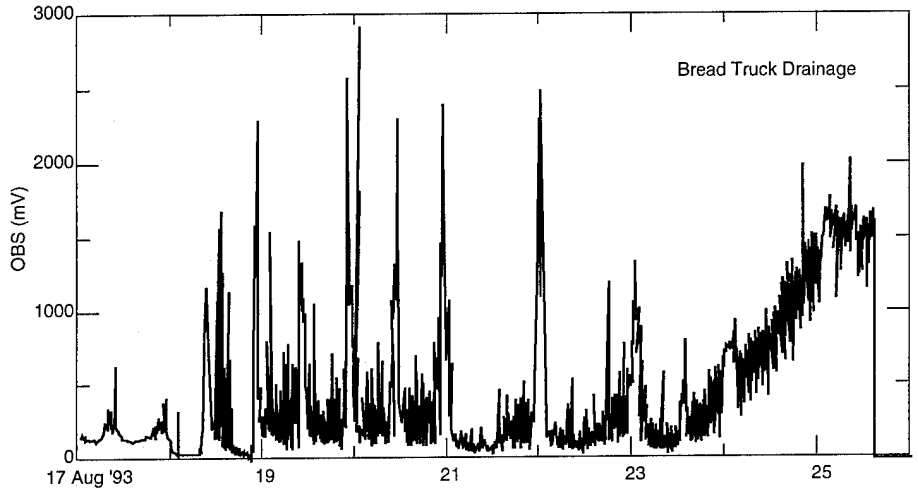


b.

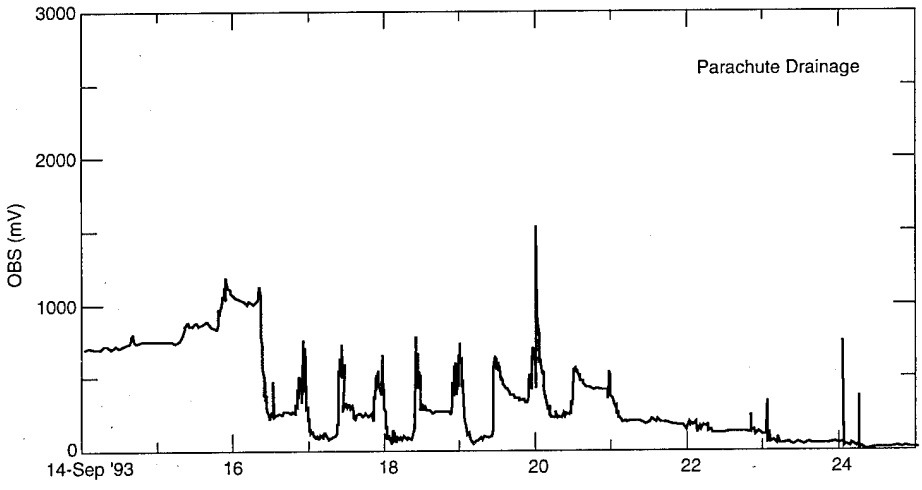


c.

*Figure 24. Optical backscatter (OBS) measurements at gully sites during August and September flooding cycles.*

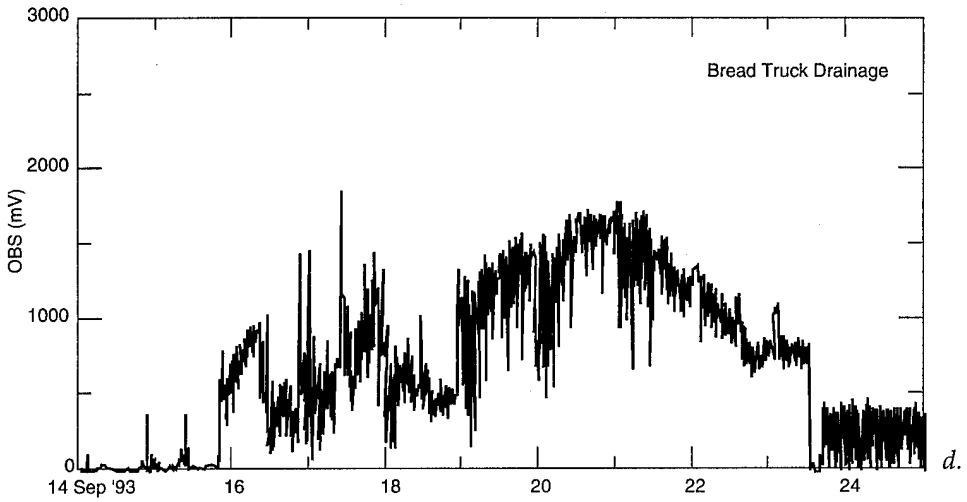


*Figure 24 (cont'd).*

on Knik Arm in September recorded peak values ranging from 1400 to 1800 mV (560 to 720 FTU). OBS readings were not obtained at Eagle River, however, owing to a lack of equipment.

As stated previously, the sporadic peaks in OBS turbidity at both gully sites may be important indicators of erosion in the gully headwall region, but vegetation or other objects in the ebb discharge can cover the sensor and cause a false indication of higher turbidity. It should be noted that because the withdrawal point for the suction sampler and the view of the OBS sensor are not precisely the same location, local increases in suspended sediment by scour or bank failure may not be sampled by the suction technique. In addition, the optical character of the water may

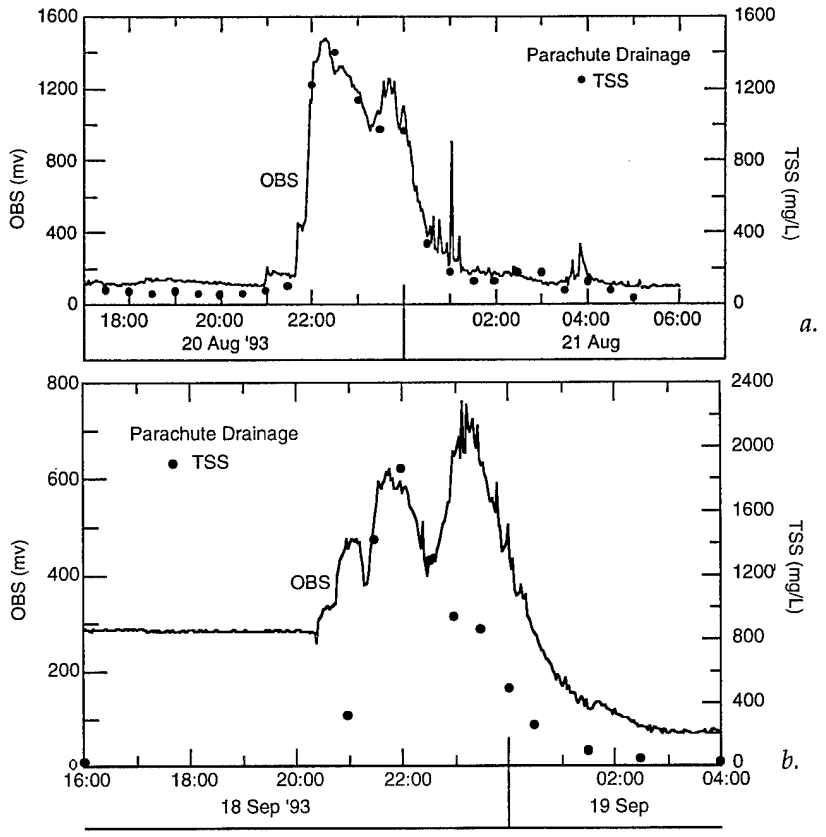


*Figure 25. Comparison of OBS and TSS measurements at Parachute Pond.*

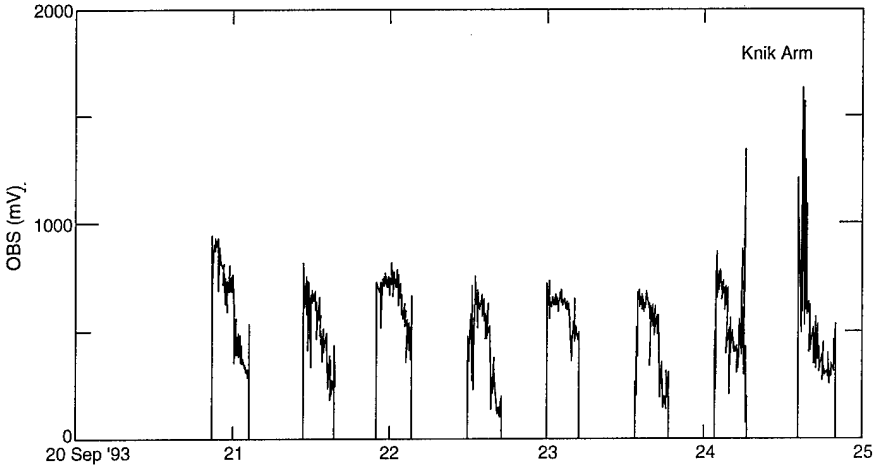


*Figure 26. OBS measurements from Knik Arm during late September.*

not always relate directly to the weight of solids present.

We attempted to calibrate OBS sensor readings of backscatter to suspended sediment concentrations using the TSS measurements. In a few events, correlations were good (Fig. 25a). However, in others, there is not a simple relationship between the two values. For example, secondary peaks in OBS readings were observed during ebb tide at the Parachute site without correspondingly high TSS values (Fig. 25b). Regression analysis of this relationship produced low correlation coefficients. A possible explanation for the secondary peaks is that, if extremely fine material is in transport during ebb, it can cause a large amount of optical backscatter, but add little to the total weight of suspended solids. This problem remains under investigation.

## SEDIMENT SOURCES

The suspended sediment concentrations measured during August and September suggest that the tidal flood waters of Knik Arm have greater concentrations of sediment in suspension than do those in the Eagle River. TSS measurements preceding, during and following tidal flooding cycles at both the Bread Truck and Parachute gully sites are consistently higher than those in the Eagle River and are similar in range to those of Knik Arm. TSS data for the Eagle River reveal concentrations ranging from 23 to 275 mg/L for 25 August to 20 September. Concentrations in two samples from Knik Arm at the coastal site were much higher: 1116 and 1273 mg/L. OBS turbidity data for 20 to 24 September at the coast also were consistently high, while the TSS samples from the river yielded much lower values (less than 100 mg/L) (Fig. 26).

Further samples are clearly needed to determine if the relationship of sediment concentration for the river and tidal sources is representative of the entire year, especially because of the inherent seasonal variability in the Eagle River's glacial sources. Sediments in Knik Arm waters are, however, also derived from glacierized basins feeding the Susitna, Knik, Matanuska and other rivers that drain into Cook Inlet and thus the tidal source may also vary seasonally.

## EROSION DYNAMICS AND GULLY HYDRAULICS

Longitudinal cross sections of the gullies, surveyed along their central channel or thalweg, have several characteristics in common. Each of the nine gullies in the study area has moderate to relatively steep slopes downstream of an eroding headwall (Fig. 27). The headwall region is characterized by a nearly vertical face ranging from 1.2 to over 2.0 m in height, at the base of which is a depression or plunge pool scoured by water flowing over the headwall (Fig. 27). This plunge pool ranges in depth from about 0.5 to over 2.0 m.

Channel gradients are steepest near the Eagle River (0.01 to 0.02 m/m). The steep bed slope probably results from the large range in tidally controlled variations in water level and discharge in the river proper. Upstream of this steep section, the gradient becomes shallower (0.003 to 0.007 m/m), but then progressively steepens with distance to the base of the headwall (Fig. 27). At one or more locations within

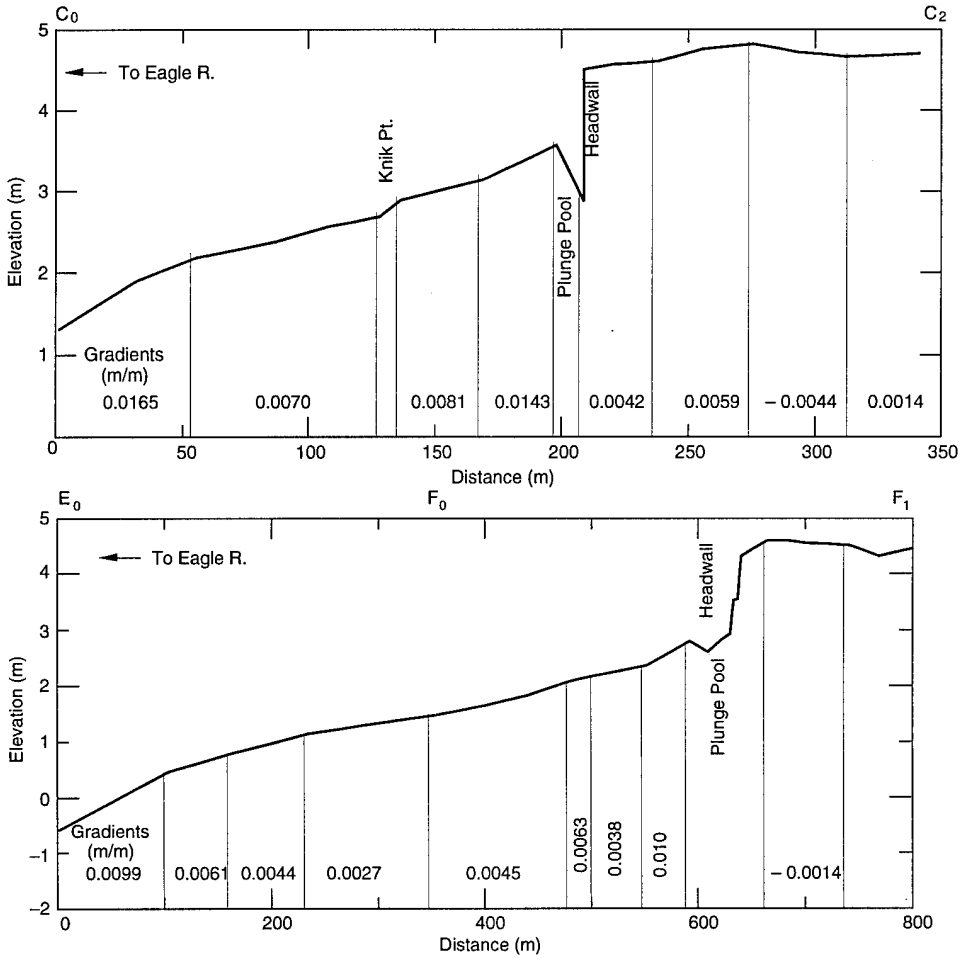


*Figure 27. Profiles of elevations along gully thalwegs of two drainages with calculated gradients indicated (see Fig. 10). Top–Gully C, bottom–Gully E.*

the gully, short segments of the channel have sharp increases in gradient. These locations, which we call knickpoints, may indicate that the bed profile is not in equilibrium with the existing hydrological conditions and that the bed slope and elevation are actively being modified by scour during flood or ebb. Such a progressive deepening of the gully thalweg and reduction in the channel gradient may be in response to the on-going headwall erosion and extension of each gully into the mudflats.

Channels above each headwall are lined by vegetation and their bed slopes range from 0.001 to 0.004 m/m, generally being less than the gradients within the gully proper. With distance, slopes gradually reverse in direction and dip upstream across the unvegetated mudflats next to the ponds.

Both the relatively rapid erosion and extension of the gully system and their relatively steep gradient suggest that the drainage system

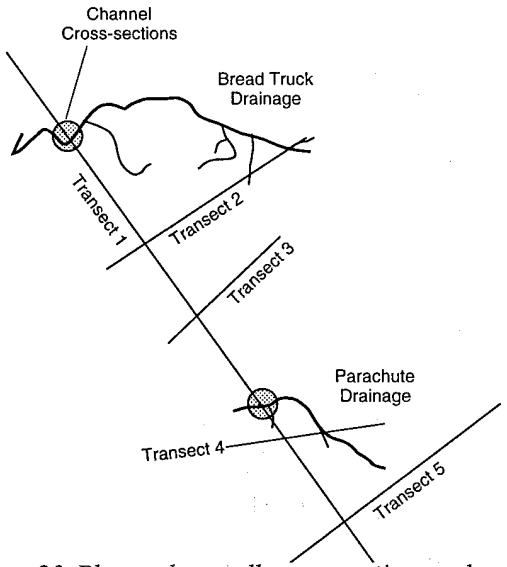


*Figure 28. Places where gully cross sections and peak flow were estimated (intersection of gully and transect 1). Figure 4 shows their location within the study area.*

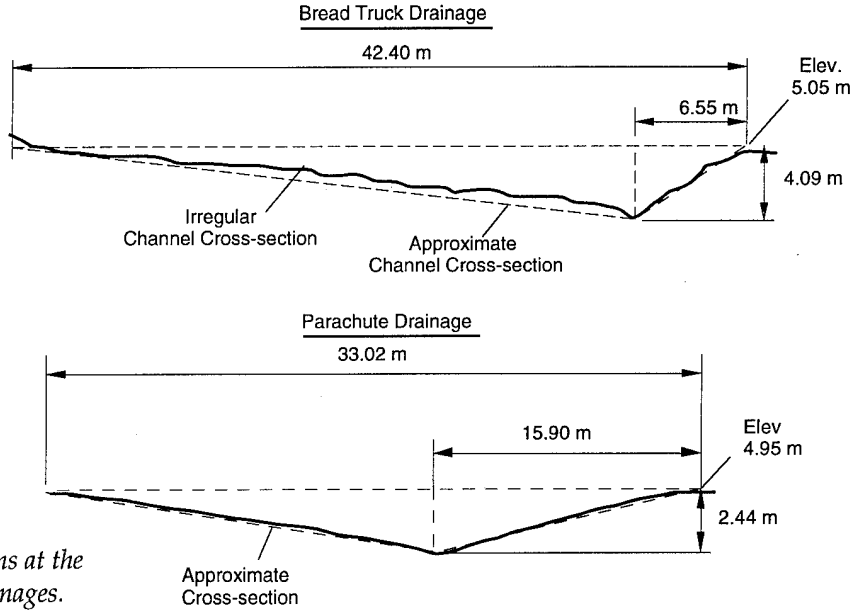


*Figure 29. Idealized cross sections at the Bread Truck and Parachute drainages.*

is actively changing. The reasons for this activity are not yet clear. Hydraulic and geotechnical forces are clearly causing such changes, but their relationship to the dynamics of the entire system remains unknown. Basic parameters such as current velocity, discharge and channel geometry need to be measured accurately to define the gullies' roles in tidal flat hydrology.

To evaluate the potential magnitude and relative importance of forces causing erosion and sediment transport within the gullies, empirical equations were used to estimate hydraulic parameters for peak flow during ebb. Gully profiles, bank elevations and calculated slopes for the Bread Truck and Parachute drainages were used to approximate the shape of the drainage cross section and estimate maximum velocities and discharge (Fig. 28 and 29).

Sediment transport and gully erosion are primarily related to the flow velocity. Gully longitudinal profiles and cross sections were measured for the Bread Truck and Parachute drainages in an attempt to determine flow velocities in these channels. Figures 28 and 29 are representative sectional shapes that expand in each gully as one proceeds downstream.

The Manning equation was used to calculate the average flow velocity $V$ in the gully.

$$V = 1.0/N\, R^{2/3}\, S^{1/2} \qquad (1)$$

where $N$ = Manning coefficient (0.018 for clean earth)
$R$ = hydraulic radius
$S$ = slope.

**Table 5. Gully parameters.**

| *Location* | A ($m^2$) | $P_w$ (*m*) | R (*m*) | S (*m/m*) | N |
|---|---|---|---|---|---|
| Bread Truck drainage | 86.7 | 43.8 | 1.98 | 0.0044 | 0.018 |
| Parachute drainage | 40.3 | 33.4 | 1.21 | 0.0062 | 0.018 |

Table 5 gives values of the above parameters, as well as area ($A$) and wetted perimeter ($P_W$). We assumed that the depth of flow was at bankfull stage and that the channel slope in the gully was in uniform flow. These calculations produced very high flow velocities (more than 4.5 m/s) and Froude numbers in excess of 1.0. Since these values indicate supercritical flow, the flow must undergo a hydraulic jump to a greater depth, which is not possible for the assumed bankfull conditions. Thus, simplifying the hydraulic conditions to a uniform flow assumption is not feasible for currents within the gullies.

Obviously, these flow velocity calculations are not representative of the actual situation and more detailed information on the hydraulic controls (downstream and upstream) or actual velocity measurements are needed. Our observations suggest flow velocities are actually in the 1–3 m/s range during ebb.

## EROSION AND RECESSION RATES

Erosion of gully headwalls is causing their progressive elongation into the mudflats and presumably into the ponds. Rates of recession of the gully headwall and adjacent lateral walls were measured at 11 sites established in 1992 and at 3

additional sites established in 1993 (Fig. 8). Net recession rates were measured between 28 May and 22 September 1992, 22 September 1992 and 2 June 1993, and 2 June and 22 September 1993, while measurements on 26 August and on 22 September 1993 permit comparison of erosion and recession resulting from a single month's cycle of flooding tides (Appendix A).

The amount of recession of the scarp crests was highly variable within a gully, as well as among the sites (Table 6). Maximum recession rates ranged from 0.1–4.9 m during May to September 1992 , 0.4–6.3 m during September 1992 to June 1993, and 0.0–9.8 m during June to September 1993 (Table 6).

At each site, however, some parts of the scarp crests did not retreat at all. This spatial variability in recessional rates is evident in plots of the scarp crest location with time (Fig. 30). Recession rates for the September 1993 flooding cycle were a maximum of 1.4 m. The extreme rate of change of 45 m was generated by the development of a new network of shallow (0.5 m) gullies in the mudflats between C and Bread Truck ponds during the 1992–93 winter (Fig. 30c).

The variability in recession rate reflects the nature of the erosional processes in causing rapid short-term changes (Table 2). Recession appears to be caused mostly by current erosion of the lower, unvegetated part of the near-vertical gully walls during ebb. Because the uppermost 20 to 30 cm of material is consolidated and rootbound, this soil and root mat are undermined by current erosion and only fail after an erosional niche of approximately 0.5 m or deeper is cut below it.

Eroded sediments form deposits within the gullies and are eventually transported down-gully into the Eagle River. Along steep scarps, blocks of consolidated sediments bound by roots fall and roll into the gully bottoms where currents eventually may break them down by scour or by rolling them along the gully bed. The lateral walls of gullies, which tend to develop low angle slopes as headwalls recede inland, fail mainly by retrogressive slump flow, the lower half or more of the slope creeping slowly as a mudflow into the gully channel. On gentler slopes, blocks of rootbound material remain intact as they are transported downslope by slow-moving mudflows that are active in the latter stages of the ebb cycle. Because this sequence of events happens at different times and rates, recession varies within as well as among the study sites (Table 6).

If our measurements of recession rate are characteristic, erosion will cause increased drainage of ponds within the next 10 to 15 years. Two ponds in particular will likely be affected: one is Bread Truck, on its northern side, and the other is the pond complex between the Bread Truck and C ponds (Fig. 5). Further analyses of recession rates are needed to determine if the 1992 to 1993 rates are representative of more than this 1-year period.

**Table 6. Headwall recession rates in 1992 and 1993.**

| Erosion site | Location | | Recession range (m) May–Sept 92 | | Sept 92–June 93 | | June-Sept 93 | |
|---|---|---|---|---|---|---|---|---|
| | Drainage | Position* | Min | Max | Min | Max | Min | Max |
| 1 | B† | L | 0.0 | 2.1 | 0.3 | 3.2 | 0.1 | 3.9 |
| 2 | B | L | 0.0 | 4.9 | 0.0 | 2.0 | 0.0 | 1.2 |
| 3 | C | L | 0.0 | 0.6 | 0.0 | 0.9 | 0.0 | 0.0 |
| 4 | C | H | 0.1 | 3.1 | 0.5 | 1.5 | 0.0 | 3.8 |
| 5 | C | L | 0.0 | 1.3 | 0.0 | 0.8 | 0.0 | 0.2 |
| 6 | D—S. Fork | L | 0.1 | 2.4 | 0.0 | 0.6 | 0.0 | 1.1 |
| 7 | D—S. Fork | H | 0.0 | 1.1 | 0.0 | 0.4 | 0.0 | 0.8 |
| 8 | D—Cent. Fork | L | 0.0 | 0.1 | 0.0 | 1.0 | 0.0 | 0.4 |
| 9 | D—Cent. Fork | H | 0.0 | 0.5 | 0.1 | 6.3** | 0.0 | 9.8 |
| 10 | D—Cent. Fork | L | 0.0 | 0.2 | 0.0 | 0.5 | 0.0 | 0.0 |
| 11 | D—N. Fork | L | 0.0 | 0.5 | 0.0 | 0.4 | 0.0 | 1.0 |
| 12 | F | L | — | — | — | — | 0.0 | 3.1 |
| 13 | F | L | — | — | — | — | 0.1 | 1.8 |
| 14 | F | L | — | — | — | — | 0.0 | 1.2 |

* L = lateral wall, H = headwall.

† See Figure 8.

** 45-m shallow erosion extending into mudflats (Fig. 30).

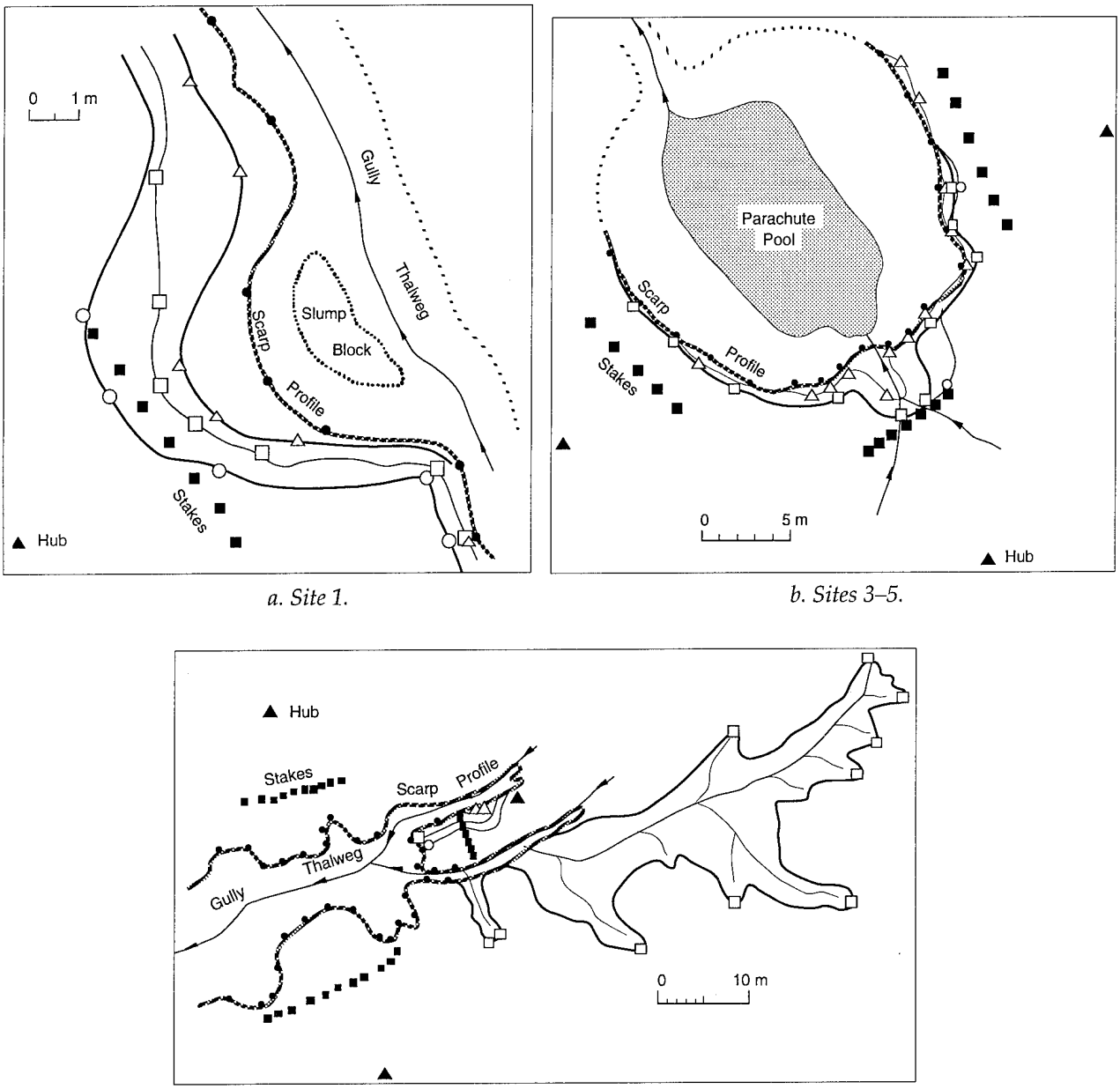


*a. Site 1.*

*b. Sites 3–5.*

*c. Sites 8–10.*

*Figure 30. Examples of spatial variation in erosion rates measured at gully headwall sites. Only changes are shown by symbols.*

Measured Points

- ● Original (27 May '92)
- △ Summer 1 (22 Sep '92)
- □ Winter ( 2 Jun '93)
- ○ Summer 2 (22 Sep '93)

## SEDIMENTATION RATES

Sedimentation rates vary with morphological unit and, in a general sense, with elevation. The overall trend is an increase eastward from the Eagle River levees, across the mudflats and into the ponds. Marshes, however, apparently had lower accretion rates than the ponds (Table 7), while within gullies, rates could far exceed these values. Lower sedimentation rates in marshes may reflect problems in sampling within the thick sedges, including an unknown amount trapped in the vegetation, rather than the actual rate of accretion.

The relationship of rate to elevation is in part a response to the number of times sites are inundated, but other factors appear important as well. Assuming a general elevation of 4.6 m for

**Table 7. Gross sedimentation rates in 1992 and 1993.**

| Morphological unit | Range (mm) Summer 92 | Winter 92–93 | Summer 93 |
|---|---|---|---|
| Levee | 1–2 | 1–5 | 1–5 |
| Vegetated upper mudflat | 3–6 | 3–10 | 1–8 |
| Unvegetated lower mudflat | 5–12 | 7–12 | 3–10* |
| Pond—plate | 18–35 | 8–28 | 2–12 |
| Pond—cup | | 5–38 | 6–15 |
| Marsh | 2–10 (est) | ND† | ND |
| Gully | 100–300 | 28–75** | 60** |

* Larger values from craters.
† ND = no data.
** Based on small sample size.

**Table 8. Number of flooding events reaching critical heights to cover landforms in 1992 and 1993.**

| Critical height | Number of flooding events Summer 92 | Winter 92–93 | Summer 93 |
|---|---|---|---|
| Ponds (4.6 m) | 21 | 66 | 23 |
| Mudflats (4.87 m) | 13 | 36 | 15 |
| Levees (5.21 m) | 2 | 9 | 4 |

ponds to flood (a 9.48-m Anchorage datum tide), Table 8 shows a minimum of 21 sediment-bearing tidal floodings would have filled ponds, mainly during the late July to early August and late August to early September tidal cycles. Through September 1992 to May 1993, the ponds were inundated by a minimum of 66 sediment-bearing tides monthly (except December), with the highest tides in March and April. Although there may have been additional flooding during summer because of higher discharges, the range in sedimentation rates for ponds during the winter with more flooding tides was similar to that of the previous summer (1 to 38 mm). This similarity may reflect several other factors, including lower sediment concentrations in winter flood waters, or ice cover effects, such as the freeze-on and removal of pond bottom sediments during freezeup or breakup. From May to September 1993, 23 sediment-bearing floods occurred, mainly from July through September. These rates were generally lower than in either the summer or winter of 1992, ranging from 1 to 15 mm. The reasons for these reduced rates are not yet known.

Gross sedimentation rates were higher within ponds than on river levees (Table 7); this appears related to the total number of flooding events covering each landform. During the entire period, 110 tides exceeded the 4.6-m elevation necessary to enter the ponds (Table 8). In contrast, levee elevation data suggest that during the same period, only 15 tides were sufficiently high to inundate them completely. The average sediment accumulation in the ponds from May 1992 to September 1993 was 46.5 mm, yielding a gross rate per tidal cycle of 0.4 mm. The average rate per tidal flooding on levees is 0.3 mm.

The higher rates of sedimentation in ponds than on river levees clearly show the more important role of tidal inundation than Eagle River floods as a sediment source and thus, within the study area, sedimentation is tidally dominated. The large amount of suspended sediment in Knik Arm increases its importance relative to the Eagle River, and contrasts with other tidally dominated salt marshes and mudflats where glaciers are not important sources of marine suspended sediments. The role of the river is lessened by its apparently lower suspended sediment transport rate, including the lack of sediment influx during winter.

The amount of material that originated by resuspension of pond bottom sediments ranged from 8 to 16 mm for the summer of 1992, or approximately equivalent to the thickness of new sediments deposited in the ponds during the same period (Table 7). During the late August to early September flooding cycle, 3–6 mm of new

material was deposited, while 2–6 mm of material had been resuspended and redeposited. During the winter 1992–93 period, resuspension sedimentation ranged from 2 to 15 mm, or similar to that of the summer 1993 amounts.

Within gullies, deposition occurs mainly along the lateral slopes away from the channel thalweg. Depending on the depositional process, rates could range as high as 10 to 30 cm for the summer period, with several or more centimeters being deposited during a single flood and ebb cycle. These rates primarily reflect adjustments in the gully cross section, rather than deposition from tidal flood waters. Mass movements of slope material account for the majority of the sediment deposited on lateral slopes. Sedimentation rates are therefore highly variable from place to place. Note that the 1992–93 winter and 1993 summer gully measurements are not directly comparable to the 1992 summer measurements because most of the 1992 stakes within the center of the gully were lost to erosion or burial.

## SYSTEM DYNAMICS AND REMEDIATION

Eagle River Flats is a dynamic estuarine salt marsh that is actively undergoing progressive and significant changes in the physical environment. These changes result from the interaction of multiple physical processes with various factors that include external forces such as a high tidal range, a glacial river, two relatively large sediment sources and a cold climate. The location of ERF within an active earthquake zone adds further to the complexity and the potential for future rapid, but probably unpredictable, physical changes. If the area subsides, or conversely uplifts, because of an earthquake, major changes in the hydrology and terrain can be expected. While pond areas may increase because of subsidence, as happened in 1964, the drainage system and river channel may respond with increases in rates of erosion or sedimentation because the drainageways will be out of equilibrium with the altered physical environment. In addition, ground explosions and cratering during the use of ERF as a military firing range since the early 1940s have caused physical changes to the terrain, hydrology and surface drainage. Craters, for example, have locally increased erosion in drainages and enhanced gully expansion.

The inherent complexity of this dynamic environment makes it extremely difficult to predict what effects potential remedial measures for WP contamination will have on the physical system and conversely what short- and long-term effects the physical system will have on the effectiveness and success of proposed remedies. Understanding both the system's response and the effects of remedial measures are critical to developing cleanup strategies. Further analysis of the processes and factors determining tidal flat hydrology and sedimentology are required to predict the system's response to a particular remedial technology. The remediation process may be enhanced or hindered by the physical system. Questions regarding remediation will be addressed in our continuing investigations of the physical system dynamics of Eagle River Flats.

## LITERATURE CITED

**Andrew, J. and G. Cooper** (1993) Sedimentation in a river dominated estuary. *Sedimentology*, **40**: 979–1017.

**Allen, J.R.L.** (1982) Sedimentary structures: Their character and physical basis. In *Developments in Sedimentology*, vol. 30A, B. New York: Elsevier.

**Allen, J.R.L.** (1990a) Constraints on measurements of sea-level movements from salt marsh accretion rates. *Journal of the Geological Society, London*, **147**: 5–7.

**Allen, J.R.L.** (1990b) Salt marsh growth and stratification: A numerical model with special reference to Severn Estuary, southwest Britain. *Marine Geology*, **95**: 77–96.

**Allen, J.R.L.** (1992) Large-scale textural patterns and sedimentary processes on tidal salt marshes in Severn Estuary, southwest Britain. *Sedimentary Geology*, **81**: 299–318.

**Allen, J.R.L. and J.E. Rae** (1988) Vertical salt marsh accretion since the Roman period in the Severn Estuary, southwest Britain. *Marine Geology*, **83**: 225–235.

**Bartsch-Winkler, S. and A.T. Ovenshine** (1984) Macrotidal subarctic environment of Turnagain and Knik Arms, Upper Cook Inlet, Alaska: Sedimentology of the intertidal zone. *Journal of Sedimentary Petrology*, **54**: 1221–1238.

**Bloom, A.L.** (1984) Peat accumulation and compaction in a Connecticut coastal marsh. *Journal of Sedimentary Petrology*, **34**: 599–603.

**Boon, J.D.** (1975) Tidal discharge asymmetry in a salt marsh drainage system. *Limnology and Oceanography*, **20**: 71–80.

**Carling, P.A.** (1981) Sediment transport by tidal currents and waves: observations from a sandy intertidal zone (Burry Inlet, South Wales). In *Holocene Marine Sedimentation in the North Sea Basin* (S.D. Nio, R.T.E. Schüttenhelm and Tj.C.E. van Weering, Ed.). I.A.S. Special Publication **5**: 65–80.

**Carling, P.A.** (1982) Temporal and spatial variation in intertidal sedimentation rates. *Sedimentology*, **29**: 17–23.

**Collins, L.M., J.L. Collins and L.B. Leopold** (1987) Geomorphic processes of an estuarine marsh: preliminary results and hypotheses. *International Geomorphology 1986*, p. 1049–1072.

**Dalrymple, R.W., B.A. Zaitlin and R. Boyd** (1992) Estuarine facies models: conceptual basis and stratigraphic implications. *Journal of Sedimentary Petrology*, **62**: 1130–1146.

**Dionne, J.C.** (1988) Characteristic features of modern tidal flats in cold regions. In *Tide-Influenced Sedimentary Environments and Facies* (P.L. deBoer, A. van Gelder and S.D. Nio, Ed.). Boston: D. Reidel Publishing Company, p. 301–332.

**Evans, C.D., E. Buch, R. Buffler, G. Fish, R. Forbes and W. Parker** (1972) The Cook Inlet environment: A background study of available knowledge. University of Alaska Sea Grant Program.

**French, J.R.** (1991) Eustatic and neotectonic controls on saltmarsh sedimentation. In *Coastal Sediments '91* (N.C. Kraus, K.J. Gingerich and D.L. Kriebel, Ed.). New York: American Society of Civil Engineers, p. 1223–1236.

**French, J.R.** (1993) Numerical simulation of vertical marsh growth and adjustment to accelerated sea-level rise, north Norfolk, U.K. *Earth Surface Processes and Landforms*, **18**: 68–81.

**French, J.R. and T. Spencer** (1993) Dynamics of sedimentation in a tide-dominated backbarrier salt marsh, Norfolk, U.K. *Marine Geology*, **110**: 315–331.

**Frostick, M.E. and I.N. McCave** (1979) Seasonal shifts of sediments in an estuary mediated by algal growth. *Estuarine, Coastal and Shelf Science*, **9**: 569–576.

**Gurnell, A.M. and J.C. Clark, Ed.** (1987) *Glacio-Fluvial Sediment Transfer*. New York: John Wiley and Sons.

**Hanson, H.C.** (1951) Characteristics of some grassland, marsh and other plant communities in western Alaska. *Ecological Monographs*, **21**: 327–378.

**Harrison, E.Z. and A.L. Bloom** (1977) Sedimentation rates on tidal salt marshes. *Journal of Sedimentary Petrology*, **47**: 1484–1490.

**Hubbard, J.C.E. and R.E. Stebbings** (1968) Spartina marshes in southern England III. Stratigraphy of the Keyworth marsh, Poole Harbour. *Journal of Ecology*, **56**: 707–722.

**Kearney, M.S. and L.G. Ward** (1986) Vertical accretion rates in brackish marshes of a Chesapeake Bay tributary. *Geo-Marine Letters*, **6**: 41–49.

**Keene, H.W.** (1971) Postglacial submergence and salt marsh evolution in New Hampshire. *Maritime Sediments*, **7**: 64–68.

**Kohsiek, L.H.M., J. Alphen, P. Bloks and P. Hoekstra** (1981) A water and sediment balance of a salt marsh in the Eastern Scheldt Estuary (Research Rept. RWS Nr. DDWT 81.042).

**Krone, R.B.** (1987) A method for simulating historic marsh elevations. In *Coastal Sediments '87* (N.D. Krause, Ed.). New York: American Society of Civil Engineers, p. 316–323.

**Lawson, D.E.** (1993) Glaciohydrologic and glaciohydraulic effects on runoff and sediment yield in glacierized basins. USA Cold Regions Research and Engineering Laboratory, Monograph 93–2.

**Lawson, D.E. and B.E. Brockett** (1993) Preliminary assessment of sedimentation and erosion in Eagle River Flats, southcentral, Alaska. USA Cold Regions Research and Engineering Laboratory, CRREL Report 93–23.

**Leopold, L.B., M.G. Wolman and J.P. Miller** (1964) *Fluvial Processes in Geomorphology*. San Francisco: W.H. Freeman, Co.

**Letzch, W.S. and R.W. Frey** (1980) Deposition and erosion in a Holocene salt marsh. *Journal of Sedimentary Petrology*, **50**: 529–542.

**McCann, S.B., J.E. Dale and P.B. Hale** (1981) Subarctic tidal flats in areas of large tidal range, southern Baffin Island, eastern Canada. *Geographie Physique et Quaternaire*, **35**: 183–204.

**McLaren, P., M.B. Collins, S. Gao and R.I.L. Powys** (1993) Sediment dynamics of the Seven Estuary and Inner Bristol Channel. *Journal of the Geological Society of London*, **50**: 589–603.

**Ovenshine, A.T., D.E. Lawson and S.R. Bartsch-Winkler** (1976a) The Placer River silt: An intertidal deposit caused by the 1964 Alaskan earthquake. *Journal of Research, U.S. Geological Survey*, **4**: 151–162.

**Ovenshine, A.T., S.R. Bartsch-Winkler, N.R. O'Brien and D.E. Lawson** (1976b) Sediment of the high tidal range environment of upper Turnagain Arm, Alaska. In *Recent and Ancient Sedimentary Environments in Alaska* (T.P. Miller, Ed.). Memoir, Alaskan Geological Society, p. M–1 to M–26.

**Racine, C.H., M.E. Walsh, C.M. Collins, D.J. Calkins, B.D. Roebuck and L. Reitsma** (1992a) Water-

fowl mortality in Eagle River Flats, Alaska. USA Cold Regions Research and Engineering Laboratory, CRREL Report 92–5.

**Racine, C.H., M.E. Walsh, B.D. Roebuck, C.M. Collins, D. Calkins, L. Reitsma, P. Buchli and G. Goldfarb** (1992b) White phosphorus poisoning of waterfowl in an Alaskan salt marsh. *Journal of Wildlife Diseases*, **28**(4): 669–673.

**Racine, C.H., M.E. Walsh, C.M. Collins, D. Lawson, K. Henry, L. Reitsma, B. Steele, R. Harris and S.T. Bird** (1993) White phosphorus contamination of salt marsh sediments at Eagle River Flats, Alaska. USA Cold Regions Research and Engineering Laboratory, CRREL Report 93–17.

**Reed, D.J.** (1990) The impact of sea-level rise on coastal salt marshes. *Progress in Physical Geography*, **14**: 465–481.

**Richard, G.A.** (1978) Seasonal and environmental variations in sediment accretion in a Long Island salt marsh. *Estuaries*, **1**: 29–35.

**Rosenberg, D.H.** (1986) Wetland types and bird use of Kenai Lowlands. Anchorage, Alaska. U.S. Fish and Wildlife Service, Special Studies.

**Röthlisberger, J. and H. Lang** (1987) Glacial hydrology. In *Glacio-Fluvial Sediment Transfer* (A.M. Gurnell and J.C. Clark, Ed.). New York: John Wiley and Sons, p. 207–284.

**Stoddart, D.R., D.J. Reed and J.R. French** (1989) Understanding salt marshes. *Estuaries*, **12**: 228–236.

**Small, J.B. and L.C. Wharton** (1969) Vertical displacements determined by surveys after the Alaska earthquake of March 1964. The Prince William Sound, Alaska, earthquake of 1964 and aftershocks. In *Research Studies and Interpretive Results, Geodesy and Photogrammetry* (L.E. Leipold and F.J. Wood, Ed.). Washington, D.C.: U.S. Coast and Geodetic Survey, Volume III, p. 21–33.

**USGS** (1981) Water resources data for Alaska, water year 1980. U.S. Geological Survey Water Resources Division, Annual Report for Alaska. USGS/WRD/HD-81/004 and USGS/WRD/AK-80-1.

**Vince, S.W. and A.A. Snow** (1984) Plant zonation of an Alaskan salt marsh. II. An experimental study of the role of edaphic conditions. *Journal of Ecology*, **72**: 669–684.

# APPENDIX A: RECESSION RATE SUMMARY
## (sites located on Figure 8)

| Hub | Stake | Erosion rate (m) Summer '92 | Winter | Summer '93 |
|---|---|---|---|---|
| **Drainage B** | | | | |
| *Site 1 (established 27 May 92)* | | | | |
| B | 28 | 1.3 | 2.1 | 3.9 |
| | 96 | 1.3 | 3.2 | 2.1 |
| | 26 | 2.1 | 0.6 | 0.6 |
| | 98 | 1.3 | 0.5 | 0.9 |
| | 29 | 0.6 | 0.9 | 0.9 |
| | 97 | 0.0 | 0.6 | 0.1 |
| | 27 | 0.0 | 0.3 | 0.3 |
| | Min | 0.0 | 0.3 | 0.1 |
| | Max | 2.1 | 3.2 | 3.9 |
| *Site 2 (established 27 May 92)* | | | | |
| A | 92 | 0.0 | 0.1 | 0.0 |
| | 38 | 0.0 | 0.4 | 0.0 |
| | 87 | 0.1 | 0.3 | 0.6 |
| | 48 | 4.9 | 2.0 | 0.9 |
| | 86 | 0.4 | 0.0 | 0.0 |
| | 43 | 0.0 | 0.0 | 0.0 |
| | 91 | 0.1 | 0.3 | 0.3 |
| | 47 | 0.2 | 0.6 | 0.0 |
| | 93 | 0.0 | 0.4 | 0.0 |
| | 45 | 2.0 | 1.3 | 0.2 |
| | 100 | — | — | 1.2 |
| | 101 | — | — | 1.2 |
| | 102 | — | — | 0.8 |
| | Min | 0.0 | 0.0 | 0.0 |
| | Max | 4.9 | 2.0 | 1.2 |
| **Parachute gully (drainage C)** | | | | |
| *Site 3 (west side, established 27 May 92)* | | | | |
| 31 | 32 | 0.1 | 0.0 | 0.0 |
| | 81 | 0.0 | 0.4 | 0.0 |
| | 41 | 0.0 | 0.3 | 0.0 |
| | 88 | 0.6 | 0.0 | 0.0 |
| | 33 | 0.0 | 0.9 | 0.0 |
| | Min | 0.0 | 0.0 | 0.0 |
| | Max | 0.6 | 0.9 | 0.0 |
| *Site 4 (south side, established 27 May 92)* | | | | |
| 85 | 34 | 1.0 | — | — |
| | 95 | 0.8 | 0.5 | 0.0 |
| | 44 | 0.7 | — | — |
| | 80 | 3.1 | 1.5 | 0.0 |
| | 49 | 0.2 | — | — |
| | 78 | 0.1 | — | — |
| | 42 | 0.3 | 0.8 | 3.8 |
| | Min | 0.1 | 0.5 | 0.0 |
| | Max | 3.1 | 1.5 | 3.8 |
| *Site 5 (east side, established 27 May 92)* | | | | |
| 94 | 84 | 0.1 | 0.8 | 0.0 |
| | 36 | 0.1 | 0.2 | 0.2 |
| | 76 | 0.2 | 0.6 | 0.1 |
| | 40 | 0.0 | 0.1 | 0.0 |
| | 89 | 0.7 | 0.0 | 0.0 |
| | 37 | 1.3 | 0.2 | 0.0 |
| | Min | 0.0 | 0.0 | 0.0 |
| | Max | 1.3 | 0.8 | 0.2 |

| Hub | Stake | Erosion rate (m) Summer '92 | Winter | Summer '93 |
|---|---|---|---|---|
| **"In between" drainage–southern fork (drainage D)** | | | | |
| *Site 6 (west side, established 28 May 92)* | | | | |
| 64 | 57 | 2.4 | 0.0 | 0.0 |
| | 4 | 0.8 | 0.3 | 0.0 |
| | 68 | 0.1 | 0.0 | 0.0 |
| | 3 | 0.1 | 0.1 | 0.3 |
| | 71 | 0.4 | 0.1 | 1.1 |
| | 5 | 0.1 | 0.0 | 0.0 |
| | 51 | 0.9 | 0.0 | 0.0 |
| | 2 | 1.8 | 0.6 | 0.0 |
| | 56 | 1.0 | 0.3 | 0.3 |
| | Min | 0.1 | 0.0 | 0.0 |
| | Max | 2.4 | 0.6 | 1.1 |
| *Site 7 (southeast upstream side, established 28 May 92)* | | | | |
| 66 | 6 | 1.1 | 0.0 | 0.5 |
| | 61 | 0.1 | 0.2 | 0.4 |
| | 1 | 0.1 | 0.3 | 0.0 |
| | 53 | 0.0 | 0.0 | 0.0 |
| | 7 | 0.0 | 0.4 | 0.0 |
| | 52 | 0.1 | 0.2 | 0.8 |
| | Min | 0.0 | 0.0 | 0.0 |
| | Max | 1.1 | 0.4 | 0.8 |
| **"In between" drainage–central fork (drainage D)** | | | | |
| *Site 8 (east side, established 28 May 92)* | | | | |
| 13 | 65 | 0.1 | 0.0 | 0.0 |
| | 8 | 0.1 | 1.0 | 0.0 |
| | 58 | 0.1 | 0.1 | 0.4 |
| | 17 | 0.0 | 0.0 | 0.0 |
| | 60 | 0.0 | 0.4 | 0.0 |
| | 12 | 0.1 | 0.0 | 0.0 |
| | 54 | 0.1 | 0.5 | 0.1 |
| | 9 | 0.0 | 0.1 | 0.0 |
| | 62 | 0.0 | 0.0 | 0.2 |
| | Min | 0.0 | 0.0 | 0.0 |
| | Max | 0.1 | 1.0 | 0.4 |
| *Site 9 (south side, established 28 May 92)* | | | | |
| 10 | 72 | 0.0 | 0.4 | 0.0 |
| | 20 | 0.1 | 0.1 | 0.0 |
| | 73 | 0.5 | 0.1 | 0.0 |
| | 23 | 0.0 | 0.2 | 0.7 |
| | 63 | 0.0 | 0.1 | 9.8 |
| | 25 | 0.0 | 6.3 | 0.6 |
| | Min | 0.0 | 0.1 | 0.0 |
| | Max | 0.5 | 6.3 | 9.8 |
| *Site 10 (west side, established 28 May 92)* | | | | |
| 16 | 55 | 0.1 | 0.3 | 0.0 |
| | 15 | 0.1 | 0.0 | 0.0 |
| | 70 | 0.0 | 0.2 | 0.0 |
| | 18 | 0.1 | 0.1 | 0.0 |
| | 67 | 0.0 | 0.1 | 0.0 |
| | 24 | 0.2 | 0.2 | 0.0 |
| | 75 | 0.0 | 0.1 | 0.0 |
| | 22 | 0.0 | 0.1 | 0.0 |
| | 59 | 0.0 | 0.1 | 0.0 |
| | 21 | 0.1 | 0.0 | 0.0 |
| | 69 | 0.0 | 0.5 | 0.0 |
| | Min | 0.0 | 0.0 | 0.0 |
| | Max | 0.2 | 0.5 | 0.0 |

| Hub | Stake | Erosion rate (m) Summer 92 | Winter | Summer 93 |
|---|---|---|---|---|
| **"In-between drainage" - northern fork (drainage D)** | | | | |
| *Site 11 (east side, established 28 May 92)* | | | | |
| 79 | 19 | 0.0 | 0.0 | 0.0 |
| | 46 | 0.2 | 0.0 | 0.0 |
| | 39 | 0.1 | 0.0 | 0.0 |
| | 83 | 0.1 | 0.0 | 0.0 |
| | 50 | 0.1 | 0.0 | 0.0 |
| | 77 | 0.1 | 0.0 | 0.0 |
| | 14 | 0.1 | 0.0 | 0.0 |
| | 82 | 0.1 | 0.0 | 0.0 |
| | 35 | 0.1 | 0.0 | 0.1 |
| | 90 | 0.0 | 0.0 | 1.0 |
| | 11 | 0.0 | 0.0 | 0.0 |
| | 30 | 0.5 | 0.4 | 0.1 |
| | Min | 0.0 | 0.0 | 0.0 |
| | Max | 0.5 | 0.4 | 1.0 |
| **Bread Truck drainage (drainage F)** | | | | |
| *Site 12 (on southern offshoot to west, established 2 July 93)* | | | | |
| 100 | 104 | — | — | 0.5 |
| | 103 | — | — | 0.0 |
| | 102 | — | — | 0.8 |
| | 101 | — | — | 2.1 |
| | 110 | — | — | 3.1 |
| | Min | — | — | 0.0 |
| | Max | — | — | 3.1 |

| Hub | Stake | Erosion rate (m) Summer 92 | Winter | Summer 93 |
|---|---|---|---|---|
| *Site 13 (on southern offshoot to west, established 2 July 93)* | | | | |
| 109 | 105 | — | — | 1.8 |
| | 106 | — | — | 1.7 |
| | 107 | — | — | 0.1 |
| | 108 | — | — | — |
| | Min | — | — | 0.1 |
| | Max | — | — | 1.8 |
| *Site 14 (north of hydrostation, established 2 July 93)* | | | | |
| 111 | 112 | — | — | 0.0 |
| | 113 | — | — | 0.0 |
| | 114 | — | — | 0.1 |
| | 115 | — | — | 1.2 |
| | 116 | — | — | 0.4 |
| | 117 | — | — | 0.0 |
| | Min | — | — | 0.0 |
| | Max | — | — | 1.2 |

# REPORT DOCUMENTATION PAGE

*Form Approved*
*OMB No. 0704-0188*



| 1. AGENCY USE ONLY (Leave blank) | 2. REPORT DATE | 3. REPORT TYPE AND DATES COVERED |
|---|---|---|
| | March 1995 | |

4. TITLE AND SUBTITLE

Initial Analyses of Eagle River Flats Hydrology and Sedimentology, Fort Richardson, Alaska

5. FUNDING NUMBERS

6. AUTHORS

Daniel E. Lawson, Susan R. Bigl, John H. Bodette and Patricia Weyrick

7. PERFORMING ORGANIZATION NAME(S) AND ADDRESS(ES)

U.S. Army Cold Regions Research and Engineering Laboratory
72 Lyme Road
Hanover, New Hampshire 03755-1290

8. PERFORMING ORGANIZATION REPORT NUMBER

CRREL Report 95-5

9. SPONSORING/MONITORING AGENCY NAME(S) AND ADDRESS(ES)

U.S. Army Engineer District, Alaska
Fort Richardson, Alaska

10. SPONSORING/MONITORING AGENCY REPORT NUMBER

11. SUPPLEMENTARY NOTES

12a. DISTRIBUTION/AVAILABILITY STATEMENT

Approved for public release; distribution is unlimited.

Available from NTIS, Springfield, Virginia 22161.

12b. DISTRIBUTION CODE

13. ABSTRACT (*Maximum 200 words*)

The physical environment of Eagle River Flats (ERF), a subarctic tidal flat and salt marsh, is progressively changing because of the interactions of multiple physical processes, including a high tidal range, two primary sediment sources, cold climate and location within an active earthquake zone. In addition, ERF has been used by the U.S. Army as an artillery range, where high explosives or smoke-producing shells have been detonated, causing cratering and disrupting drainage. The physical environment of ERF needs to be understood to help remediate a problem of unusually high mortality rates in migrating waterfowl. This high mortality of ducks is attributable to ingestion of elemental white phosphorus (P4) particles (from smoke-producing devices), which are now distributed within near-surface sediments of the ponds and marshes. The complexity of this dynamic environment makes it extremely difficult to predict what physical effects remedial measures for the $P_4$ contamination will have and, conversely, what short- and long-term effects the physical system will have on the effectiveness and success of proposed remedies. Understanding both the system's response and the effects of remedial technologies is critical to deciding what measures are used. This report presents the initial analysis of the physical processes of erosion, sedimentation and sediment transport and the factors controlling their activity within a portion of ERF.

14. SUBJECT TERMS

Alaska
Artillery
Eagle River Flats
Hydrology
Sediments
Waterfowl mortality
White phosphorus

15. NUMBER OF PAGES
46

16. PRICE CODE

| 17. SECURITY CLASSIFICATION OF REPORT | 18. SECURITY CLASSIFICATION OF THIS PAGE | 19. SECURITY CLASSIFICATION OF ABSTRACT | 20. LIMITATION OF ABSTRACT |
|---|---|---|---|
| UNCLASSIFIED | UNCLASSIFIED | UNCLASSIFIED | UL |